AD-A143 207 PROCESSING SCIENCE TO INCREASE THE RELIABILITY OF CERAMICS(U) ROCKWELL INTERNATIONAL THOUSAND OAKS CA SCIENCE CENTER F F LANGE ET AL. JUL 84 SC5368.2FR

1/1

UNCLASSIFIED N00014-83-C-0469 F/G 11/2 NL

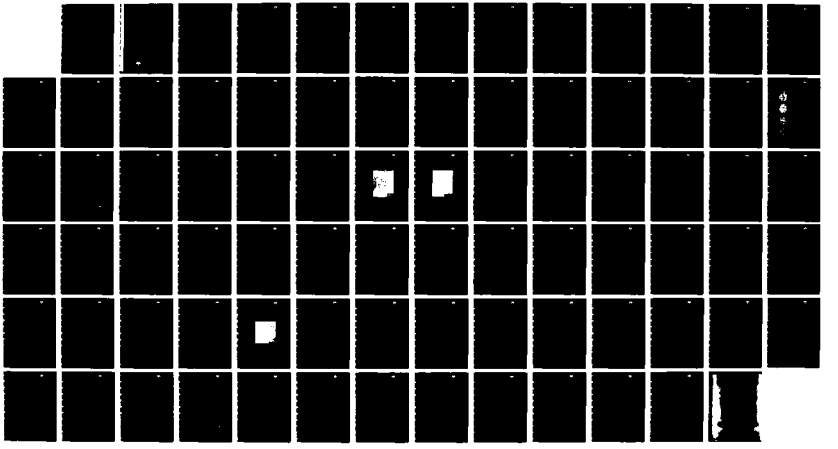

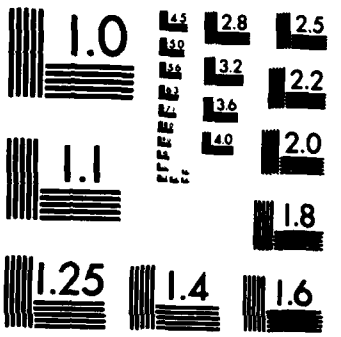

(12

SC5368.2FR

SC5368.2FR

Copy No.___

PROCESSING SCIENCE TO INCREASE THE RELIABILITY OF CERAMICS

TECHNICAL REPORT NO. 1
SINTERABILITY OF ZrO_2 AND Al_2O_3 POWDERS:
THE ROLE OF PORE COORDINATION NUMBER DISTRIBUTION

TECHNICAL REPORT NO. 2
SINTERABILITY OF AGGLOMERATED POWDERS

TECHNICAL REPORT NO. 3
EFFECT OF ZrO_2 INCLUSIONS ON THE SINTERABILITY OF Al_2O_3

TECHNICAL REPORT NO. 4
RELATIONS BETWEEN SHRINKAGE STRAIN, STRAIN RATE AND REARRANGEMENT DURING SINTERING:
EXPERIMENTAL OBSERVATIONS WITH Al_2O_3, ZrO_2 AND Al_2O_3/ZrO_2 POWDER COMPACTS

FINAL REPORT FOR THE PERIOD
June 1, 1983 through May 31, 1984

CONTRACT NO. N00014-83-C-0469
PROJECT NO. NR653-037(431)

Prepared for

Office of Naval Research
800 North Quincy Street
Arlington, VA 22217

F.F. Lange
Principal Investigator

JULY 1984

Approved for public release; distribution unlimited

Rockwell International
Science Center

UNCLASSIFIED

SECURITY CLASSIFICATION OF THIS PAGE

REPORT DOCUMENTATION PAGE

1a. REPORT SECURITY CLASSIFICATION Unclassified	1b. RESTRICTIVE MARKINGS
2a. SECURITY CLASSIFICATION AUTHORITY	3. DISTRIBUTION/AVAILABILITY OF REPORT Approved for public release; distribution unlimited.
2b. DECLASSIFICATION/DOWNGRADING SCHEDULE	
4. PERFORMING ORGANIZATION REPORT NUMBER(S) SC5368.2FR	5. MONITORING ORGANIZATION REPORT NUMBER(S)
6a. NAME OF PERFORMING ORGANIZATION Rockwell International Science Center 6b. OFFICE SYMBOL (If applicable)	7a. NAME OF MONITORING ORGANIZATION
6c. ADDRESS (City, State and ZIP Code) 1049 Camino Dos Rios Thousand Oaks, California 91360	7b. ADDRESS (City, State and ZIP Code)
8a. NAME OF FUNDING/SPONSORING ORGANIZATION Office of Naval Research 8b. OFFICE SYMBOL (If applicable)	9. PROCUREMENT INSTRUMENT IDENTIFICATION NUMBER Contract No. N00014-83-C-0469
8c. ADDRESS (City, State and ZIP Code) 800 North Quincy Street Arlington, VA 22217	10. SOURCE OF FUNDING NOS. PROGRAM ELEMENT NO. / PROJECT NO. NR653-037(431) / TASK NO. / WORK UNIT NO.
11. TITLE (Include Security Classification) PROCESSING SCIENCE TO INCREASE THE RELIABILITY OF CERAMICS (U)	
12. PERSONAL AUTHOR(S) Lange, Fred F. and Green, David J.	
13a. TYPE OF REPORT Final Report 13b. TIME COVERED FROM 06/01/83 TO 05/31/84	14. DATE OF REPORT (Yr., Mo., Day) JUNE 1984 15. PAGE COUNT 80
16. SUPPLEMENTARY NOTATION	
17. COSATI CODES FIELD / GROUP / SUB. GR.	18. SUBJECT TERMS (Continue on reverse if necessary and identify by block number)

19. ABSTRACT (Continue on reverse if necessary and identify by block number)

Technical Report No. 1: The sinterability of two ZrO_2 powders containing 2.2 and 6.6 m/o* Y_2O_3, respectively, a Al_2O_3 powder, and Al_2O_3/10 v/o* ZrO_2 composite powder was investigated. Shrinkage was measured at a constant heating rate. Capillary size distributions were determined by mercury intrusion after heating compacts to various temperatures. Iso-pressing eliminated larger pores with larger coordination numbers which results in greater sinterability. Local densification, i.e., densification of multiple-particle packing units, enlarged pores between these packing units. This phenomenon of local densification initiated prior to bulk shrinkage and stopped when the shrinkage rate reached its maximum. ZrO_2 inclusions, known to inhibit grain growth, also inhibited sinterability. This observation, coupled with previous work, strongly suggests that grain growth, supported by dense packing units, helps lower the coordination number of pores and therefore is helpful in the sintering process. Large multiple-particle packing units (large agglomerates) produce unsinterable pores, i.e., pores with high coordination numbers. It was shown that colloidal/sedimentation treatments which decrease the size of the soft and hard agglomerates reduced sintering temperatures and increased strength.

20. DISTRIBUTION/AVAILABILITY OF ABSTRACT UNCLASSIFIED/UNLIMITED ☒ SAME AS RPT. ☐ DTIC USERS ☐	21. ABSTRACT SECURITY CLASSIFICATION Unclassified
22a. NAME OF RESPONSIBLE INDIVIDUAL	22b. TELEPHONE NUMBER (Include Area Code) / 22c. OFFICE SYMBOL

DD FORM 1473, 83 APR EDITION OF 1 JAN 73 IS OBSOLETE.

UNCLASSIFIED

SECURITY CLASSIFICATION OF THIS PAGE

TABLE OF CONTENTS

LIST OF FIGURES

LIST OF FIGURES

LIST OF FIGURES

Rockwell International
Science Center

SC5368.2FR

TECHNICAL REPORT NO. 1

(In Press: Ceramic Advances, Vol. 2)

SINTERABILITY OF ZrO_2 and Al_2O_3 POWDERS: THE ROLE OF PORE COORDINATION NUMBER DISTRIBUTION

By

F.F. Lange and B.I. Davis

Rockwell International Science Center
Thousand Oaks, CA 91360

ABSTRACT

The sinterability of two ZrO_2 powders containing 2.2 and 6.6 m/o* Y_2O_3, respectively, a Al_2O_3 powder, and Al_2O_3/10 v/o* ZrO_2 composite powder was investigated. Shrinkage was measured at a constant heating rate. Capillary size distributions were determined by mercury intrusion after heating compacts to various temperatures. Iso-pressing eliminated larger pores with larger coordination numbers which results in greater sinterability. Local densification, i.e., densification of multiple-particle packing units, enlarged pores between these packing units. This phenomenon of local densification initiated prior to bulk shrinkage and stopped when the shrinkage rate reached its maximum. ZrO_2 inclusions, known to inhibit grain growth, also inhibited sinterability. This observation, coupled with previous work, strongly suggests that grain growth, supported by dense packing units, helps

*m/o = mole percent; v/o = volume percent.

lower the coordination number of pores and therefore is helpful in the sintering process. Large multiple-particle packing units (large agglomerates) produce unsinterable pores, i.e., pores with high coordination numbers. It was shown that colloidal/sedimentation treatments which decrease the size of the soft and hard agglomerates reduced sintering temperatures and increased strength.

A previous paper[1] outlined a new concept concerning the sinterability of consolidated, agglomerated powders, i.e., compacts that exhibit bulk density variations on both the macro and micro scale. Only mono-size (e.g., spherical) powders, packed with a periodic arrangement do not exhibit these density variations. Thus, nonperiodic arrangements of both mono- and polydispersed powders, spherical or otherwise, must be considered as agglomerated.

Pores are the central characters of this new concept and their coordination number (R, defined as the numer of touching particles that form the pore "surface" in the consolidated state and/or the number of surrounding grains in the partially sintered state) distribution (V(R), the function that describes the volume fraction of pores with a given R), their principal functional property. Use was made of a thermodynamic concept, first introduced by Kingery and Francois[2] and modified by Cannon,[3] which shows that pores with a coordination number less than a critical value (R_c) can shrink and disappear (kinetics permitting) by volume/grain-boundary diffusion as shown in Fig. 1a. Pores with a coordination number > R_c, will only shrink to an equilibrium size[3] as shown in Fig. 1b. The critical coordination number, R_c, depends on the dihedral angle, which depends on surface and grain boundary energies and is therefore influenced by atomic bonding and surface chemistry. Thus, from a thermodynamic viewpoint, the volume fraction of pores that can disappear is given by

$$\int_{4}^{R_c} V(R)dR \quad ,$$

where 4 is considered the lowest coordination number.

The previous paper[1] suggested that the pore coordination number distribution of a powder compact was dependent on how multiple particle packing units were arranged in space. Two types of multiple-particle packing units were visualized, i.e., domains which consisted of relatively few highly coordinated particles and thus have the lowest pore coordination distribution and agglomerates which consist of packed domains. The interdomain pores have a higher coordination number distribution than the domains themselves. The agglomerates pack together to form the powder compact. The interagglomerate pores have the highest coordination number distribution. The pore coordination number distribution is thus the sum of the distributions within the domains, between the domains, and between the agglomerates.

The effect of consolidation forces (e.g., iso-pressing) and heating on the pore coordination distribution were discussed.[1] It was suggested that consolidation forces cause the multiple-particle packing units to deform to fill in the largest pores and thus increase bulk density by removing higher coordinated pores. Increasing the bulk density increases the proportion of pores with coordination numbers $< R_c$ thus helping to explain why compacts with a higher bulk density achieve higher end-point densities for a given sintering schedule.

The effects produced during heating to temperatures where diffusional processes promote neck formation, etc., are summarized in Fig. 2. One agglomerate is shown. Domains within the agglomerate are the most highly coordinated with respect to particles (i.e., greatest number of particle contacts per volume) and contain pores with the lowest coordination number distribution. It can be shown that the free energy charge per unit volume (i.e., driving force for shrinkage) can be expressed as

$$\frac{\partial F}{\partial V} = n\gamma dA' \quad ,$$

where n is the number of contacts per unit volume ($n \alpha 1/R$), γ is the pore surface energy per unit area and dA' is the decrease in pore surface per unit compact. Domains will therefore be the first multiple particle packing unit to undergo shrinkage. Since each domain can not be expected to shrink at the same rate (both n and the V(R) within each domain will differ from domain to domain), the net effect is that domains will shrink upon themselves, breaking some interdomain necks to enlarge and increase the coordination number of interdomain pores as shown in Fig. 2b. The net effect on V(R) is to eliminate pores with a low R and increase R of other pores, i.e., a process that hinders sinterability. This process of local densification can occur without bulk shrinkage. For this case, pore volume within the domains is transferred to interdomain pores.

The multiple-connected, dense domains can now support grain growth. Grain growth (Fig. 2c) reduces the coordination number of interdomain pores. Thus, grain growth at this stage allows interdomain pores to spontaneously disappear. The end result is a dense agglomerate.

Multiple-connected agglomerates will undergo the same process as described for domains, i.e., enlargement of interagglomerate pores and grain growth to decrease the coordination number of the enlarged interagglomerate pores. The differential shrinkage between agglomerates should not be as large as that for domains since they contain many more contacts per unit volume. Bulk shrinkage is thus expected to commence with densification of agglomerates.

Thus, local densification, first of domains, then of agglomerates, increases the coordination number of the enlarged pores between the packing units. Grain growth, first supported by dense domains then by dense agglomerates, decrease the coordination number of these englarged pores. The effect of the effective compressive stress due to "surface tension" ($\sigma = \partial F/\partial V = \overline{n}\gamma dA'$) and applied compressive stresses (hot-pressing, HIPing) on reducing the coordination number of pores will not be elaborated here.

The purpose of the current paper is to review the experimental observations that appear to support the concept outlined above. These observations will be detailed for ZrO_2, Al_2O_3 and Al_2O_3/ZrO_2 powder compacts.

2.0 POWDER PREPARATION, CONSOLIDATION AND EXPERIMENTAL PROCEEDING

Two ZrO_2 powders were used, one contai..2 mole % Y_2O_3 which could be sintered to a single phase, polycrystal tetragonal ZrO_2 ceramic, and one containing 6.6 m/o Y_2O_3 which produced a cubic ZrO_2 ceramic. These powders are manufactured* by heating cellulous soaked with $ZrClO_2$ and a soluble yttrium salt in air to produce the ZrO_2 s.s. and to burn off the carbon. The hard, partially sintered agglomerates of ZrO_2 s.s. crystallites are milled and washed to remove excess chlorine. TEM examination indicated that the as-received powder still contains many large, hard agglomerates, whereas the ZrO_2 crystallites were < 0.1 μm.

The α-Al_2O_3 powder is believed to be manufactured**[4] by atomizing an alkoxide in a manner described by Visca and Matijevic.[5] The particles are nearly spherical, and the powder is claimed to have a narrow size distribution with a mean of 0.59 μm. The as-received dry powder contained many large, soft agglomerates which could be broken apart with ultrasonic treatment.

Previous work[6] showed that all three powders could be dispersed in water at pH = 2.5 (using HCl) and flocced at a pH between 7 and 9 (using NH_4OH). All three powders were subjected to a colloidal treatment outlined in Fig. 3. The purpose of this colloidal treatment was to break down soft agglomerates with the surfactant and to eliminate all hard agglomerates (or mill

*Zircar, Florida, New York, U.S.A.
**Sumitomo Chem. Co., Osaka 569 Japan (Tyoe AKP-30).

particles) > 1 μm by sedimentation. Flocculation prevents mass segregation upon storage and/or consolidation. Flocculation also consolidates the powder to a higher volume fraction. Washing to remove excess salt introduced during the disperson/flocculation steps is performed by removing the clear supernate, remixing with deionized water, and refloccing several times.

Only the ZrO_2 (+ 6.6 m/o Y_2O_3) powder was milled. A high purity* Al_2O_3 jar and media was used which introduced fractured Al_2O_3 grains (i.e., the wear product) with sizes between 5 and 20 μm. These were eliminated during sedimentation.

Figure 3 illustrates the size distribution of the three powders after redispersion. Note the bimodal distribution of the small particles and the larger hard agglomerates for the unmilled ZrO_2 (+ 2.2 m/o Y_2O_3 powder).

Two phase mixtures were prepared by determining the solid contents in each flocced system, redispersing, mixing the appropriate volumes using ultrasonics, then refloccing to prevent mass segregation.

Consolidation was performed from the flocced state by filtration (slip casting). After drying the green density of some specimens was increased by iso-pressing at 350 MPa.

Two types of air sintering experiments were performed. In the first, specimens were heated to 700°C and then heated at a constant rate of 5°C/min to 1550°C (or 1400°C for the case of ZrO_2) and then furnace cooled. Linear shrinkage was measured during these experiments with a high temperature extensiometer.

*Coors Porcelain Co.

In the second group of experiments, specimens were heated and held at the desired temperature for 30 min before furnace cooling. These specimens were then examined with a mercury porosimeter* to determine the equivalent capillary size distribution as a function of temperature.

3.0 CONSOLIDATION EFFECTS

The bulk density of the filtered ZrO_2 powders was 33% of theoretical.** It could be increased to 49% of theoretical by iso-pressing at 350 MPa. Similarly, iso-pressing of the filtered/dried Al_2O_3 powder increases the bulk density from 51% to 60% of theoretical. Figure 5 illustrates the mercury intrusion data for the filtered and filtered/iso-pressed ZrO_2 (+ 6.6 m/o Y_2O_3) powder compacts. As illustrated, the capillary size distribution is larger for the lower bulk density compact relative to the iso-pressed compact. Since the mean particle size is the same at both bulk densities, iso-pressing not only decreases the size of the larger pores, but also reduces their coordination number. That is, the compact with the higher initial bulk density is expected to contain a higher fraction of pores with coordination numbers $< R_c$.

Similar results were obtained for the other two powders.

*Micromeritics, Inc. (Auto Pore 9200)
**ZrO_2 (+ 6.6 m/o Y_2O_3), cubic structure, ρ_t = 6.05 gm/cc;
ZrO_2 (+ 2.2 m/o Y_2O_3), tetragonal structure, ρ_t = 6.07 gm/cc.

4.0 LOCAL DENSIFICATION

Local densification is a more descriptive term for what Exner[7] describes as rearrangement. As outlined above, domains will densify during the early stage of heating. Since each domain is multiple-connected to one another, but may not shrink at the same rate, void space between poorly bonded domains will enlarge. If neighboring domains exhibit sufficient differential shrinkage, pore enlargement, due to domain densification, can occur without bulk shrinkage. If a portion of the multiple-connected domains (and then, agglomerates) exhibit the same shrinkage rate, bulk shrinkage will take place during pore enlargement. An enlarged pore is less sinterable due to its increase in coordination distribution.

Figure 6 illustrates the equivalent capillary size distribution for the filtered (Fig. 6a) and filtered/iso-pressed (Fig. 6b) compacts of ZrO_2 (+ 6.6 m/o Y_2O_3) at four different temperatures. These results show (also see Fig. 5) that pore enlargement (i.e., enlargement of equivalent capillaries) precedes bulk shrinkage, viz up to 900°C. Pore enlargement continues with the initiation of bulk shrinkage at temperatures > 900°C. The process of pore enlargement stops between 1100°C and 1200°C, at which point other processes cause the large pores to shrink.

Figure 6 (and 5) also illustrates that pore enlargement takes place by a redistribution of pore sizes, viz small pores disappear* and larger pores

*Due to plotting, Fig. 6 does not show intrusion into smaller equivalent capillaries where the intrusion values are < 0.002 cc/gm.

are formed. This observation is consistent with the concept of local densification, i.e., pores within densifying domains (then agglomerates) redistributing to enlarge interdomain (or agglomerate) pores. Domain (or agglomerates) densification only leads to bulk shrinkage at temperatures > 900°C.

Figure 7 illustrates the constant heating rate, shrinkage results plotted as relative density vs temperature and shrinkage rate vs temperature. It is interesting to note that the shrinkage rate increases to its maximum at ~ 1100°C during the stage of local densification.

5.0 EFFECT OF GRAIN GROWTH

As shown previously and reviewed above, grain growth, supported by dense domains and then agglomerates, occurs throughout the sintering process. It was previously hypothesized that grain growth is helpful in reducing the coordination number of pores that would be otherwise unsinterable. To test this hypothesis, several different experiments have been initiated. One of these, which will be detailed elsewhere,[8] will be reviewed here.

Previous work[9] has shown that ZrO_2 inclusions, introduced as a second phase powder into Al_2O_3 powder, locate at 4-grain junctions during densification and hinder, but do not stop, growth of the Al_2O_3 grains. Dihedral angle measurements showed that the average Al_2O_3 grain boundary energy is ~ 1.5 times the Al_2O_3/ZrO_2 interfacial energy. One might conclude from these relative surface energies that additions of ZrO_2 to Al_2O_3 would increase the

driving force for sintering. On the other hand, if grain growth aids sintering, one might conclude that ZrO_2 additions, which hinder grain growth, would also hinder sintering.

Constant heating rate experiments were carried out for Al_2O_3 powders containing 10 vol % ZrO_2 (+ 2.2 mole % Y_2O_3) which were filtered and isopressed as described above. Results are compared with those for single phase Al_2O_3 in Fig. 8. As shown, the ZrO_2 addition delayed the start of bulk shrinkage and the maximum shrinkage rate by ~ 100°C. Note that when bulk shrinkage did initiate for the composite, it was much more rapid than for the pure Al_2O_3. These results are consistent with the hypothesis that phenomena that hinder grain growth will delay sinterability.*

Similar composites were prepared in which only a portion of the Al_2O_3 was deagglomerated (ultrasonic treatment was not employed). The resulting sintered microstructure (sintered to only 92% of theoretical) contained large, dense regions of polycrystalline Al_2O_3 without the dispersion (i.e., Al_2O_3 agglomerates which did not incorporate the ZrO_2). These dense regions contained large Al_2O_3 grains and were surrounded by lower density (porous) two-phase, finer grained matrix. This observation similarly supports the hypothesis that grain growth is helpful in decreasing the pore coordination number and thus, sinterability.

*Helpful grain growth should not be confused with abnormal grain growth which entraps pores and limits end-point density.

6.0 EFFECT OF AGGLOMERATED SIZE

The size and coordination number of an interagglomerate pore is proportional to the agglomerate size. Powders produced by decomposition reactions contain many partially-sintered, hard agglomerates. Powders consolidated by dry routes contain large, soft agglomerates. If these powders are not treated by the colloidal/sedimentation route (or a similar route) described above, these agglomerates persist through sintering.[10]

The extreme case where agglomerates are simply packed together without applied consolidation forces (no isopressing) was simulated for the Al_2O_3 powder described above. The large, soft agglomerates, collected after repeated sedimentation were consolidated by filtration. After heating to 1550°C (5°C/min, no hold time), the microstructure consisted of multiple-connected, dense agglomerates and pores as shown in Fig. 9. Since the grains within the dense agglomerates are ~ 10 times smaller, the interagglomerate pores are virtually unsinterable (without further grain growth) due to their high coordination number. Thus, powders that consist of agglomerates that are much larger then their constituent crystallites will require high sintering temperatures (despite their so-called active crystallite size) to achieve the grain growth required to reduce the coordination number of interagglomerate pores to $< R_c$. Preliminary observation currently suggest that grains have to grow to the size of the agglomerate before the interagglomerate pore can spontaneously disappear.

The highly agglomerated (hard type) ZrO_2 powders used here are a cause in point. Untreated (as-received and slightly milled), densities of 95% theoretical can only be achieved by sintering at 1600°C/2 hrs. Treated to breakup soft agglomerates and eliminate hard agglomerates > 1 μm as described above, the ZrO_2 (+ 6.6 m/o Y_2O_3) powders can be sintered to > 98% of theoretical at 1300C/1 hr. The ZrO_2 (2.2 m/o Y_2O_3) which contain a large fraction of hard agglomerates < 1 μm (see Fig. 4), can be sintered to the same density at a slightly higher temperature.

The more general case is where the larger agglomerates only make up a small fraction of the powder compact, viz the case where milling reduces a large fraction of the large agglomerates to their consistent crystallites or domains) and the compact is consolidated from the colloidal state. This case was also simulated by mixing the colloidally/sedimented Al_2O_3 with sedimented large Al_2O_3 agglomerates. As shown previously,[10] the differential shrinkage of the agglomerate relative to the matrix produce a crack-like void with a size proportional to the agglomerate as shown in Fig. 10. Again, these crack-like voids are unsinterable without either an applied pressure (e.g., or extensive grain growth). They not only limit the end-point density, but also are fracture origins that limit potential strength.

Comparison of the two ZrO_2 powders is a case in point. The unmilled ZrO_2 (+ 2.2 m/o Y_2O_3) powder contained a larger fraction of hard agglomerates (< 1 μm) than the milled ZrO_2 (+ 6.6 m/o Y_2O_3) powder after the same colloidal/sedimentation treatment (see Fig. 4). A comparison of their sintering behavior (constant heating rate of 5°C/min to 1400°C) shows (Fig. 11) that the powder

containing the large fraction of hard agglomerates achieved a lower end-point density despite the fact that they contributed to a higher shrinkage rate at lower temperatures (< 1200°C).

7.0 CONCLUSIONS

1. The thermodynamic potential of a crystalline powder compact to densify is governed by the coordination number distribution of its pore space and the critical coordination number. That is, a compact's sinterability (kinetics permitting) is determined by the arrangement of particles and multiple-particle packing units and the dihedral angle formed between a pore surface and a grain boundary.

2. Consolidation forces (e.g., iso-pressing) first eliminate pores with the highest coordination numbers (least sinterable) (see Fig. 5).

3. During neck formation, multiple-particle packing units which have the largest number of contacts per unit volume (or lowest pore coordination numbers) densify upon themselves to increase the coordination number (and size) of interpacking unit pores. This process of local densification (or rearrangement) can occur, to a limited extent, prior to bulk shrinkage, and to a

greater extent, during bulk shrinkage (Fig. 6). Pore enlargement due to local densification appears to cease when the shrinkage rate exceeds its maximum value (Figs. 6 and 7).

4. Grain growth is helpful in reducing the coordination number of those pores enlarged by local densification. When grain growth is inhibited with a dispersion of ZrO_2 particles in Al_2O_3, sinterability is also inhibited (Fig. 8).

5. The coordination number (and size) of interpacking unit pores are proportional to the size of the packing unit (Figs. 9 and 10).

The direction resulting from these conclusions only add reason to something we have already conceived. Namely, the most sinterable powders are mono-dispersed crystallites (or amorphous particles) which are densely packed in a periodic array. Lacking this utopian situation, the conclusions direct the fabricator to powder preparation and consolidation methods (e.g., those described in Section 2.0) of reducing sintering temperatures (viz reducing grain growth requirements) and reducing the size of the strength degrading crack-like pores. These methods have enabled the present authors to reduce sintering temperatures and to achieving mean flexural strengths for transformation-toughened, pressureless-sintered ceramics of 1300 MPa (185,000 psi).

8.0 ACKNOWLEDGMENTS

This work was supported by the Office of Naval Research under contract No. N00014-82-C-0341.

9.0 REFERENCES

1. F.F. Lange, "Sinterability of Agglomerated Ceramic Powders," sent to J. Am. Ceram Soc.

2. W.D. Kingery and B. Francois, "Sintering of Crystalline Oxides, I: Interaction Between Grain Boundaries and Pores," Sintering and Related Phenomena, Ed. by G.C. Kuczynske, N.A. Hooton and G.F. Gibbon, pp. 471-98, Gorden Breach (1967).

3. R.M. Cannon, "The Effects of Dihedral Angle and Pressure on the Driving Forces for Pore Growth and Shrinkage," to be published.

4. Y. Abe, S. Horikim, K. Fijimura and E. Ichiki, "High-Performance Al_2O_3 Fiber and Al_2O_3/Al Composites," Prog. in Sci. and Eng. of Comp. Proc ICCM-IV, pp. 1427-34 (1982).

5. M. Visca and E. Matijeric, "Preparation of Uniform Colloidal Dispersions by Chemical Reactions in Aerosols," *J. Colloid and Interface Sci.* 68 [2], 308-19 (1979).

6. I.A. Aksay, F.F. Lange and B.I. Davis, "Development of Uniformity in Al_2O_3/ZrO_2 Composites by the Colloidal/Filtration Route to Consolidation," J. Am. Ceram. Soc. (in press).

7. H.E. Exner, "Principles of Single Phase Sintering," Reviews on Powder Metallurgy and Physical Ceramics 1 [1-4], . 1-251 (1979).

8. F.F. Lange, T. Yamaguchi and P.E.D. Morgan, "Effect of ZrO_2 Dispersion on the Sintering of Al_2O_3," to be published.

9. F.F. Lange and M. Hirlinger, "Effect of ZrO_2 Dispersion on the Grain Growth of Al_2O_3," (to be published).

10. F.F. Lange and M. Metcalf, "Processing Related Fracture Origins: Part 2, Agglomerate Motion and Crack-Like Pore Formation Caused by Differential Sintering," J. Am. Ceram. Soc. (in press).

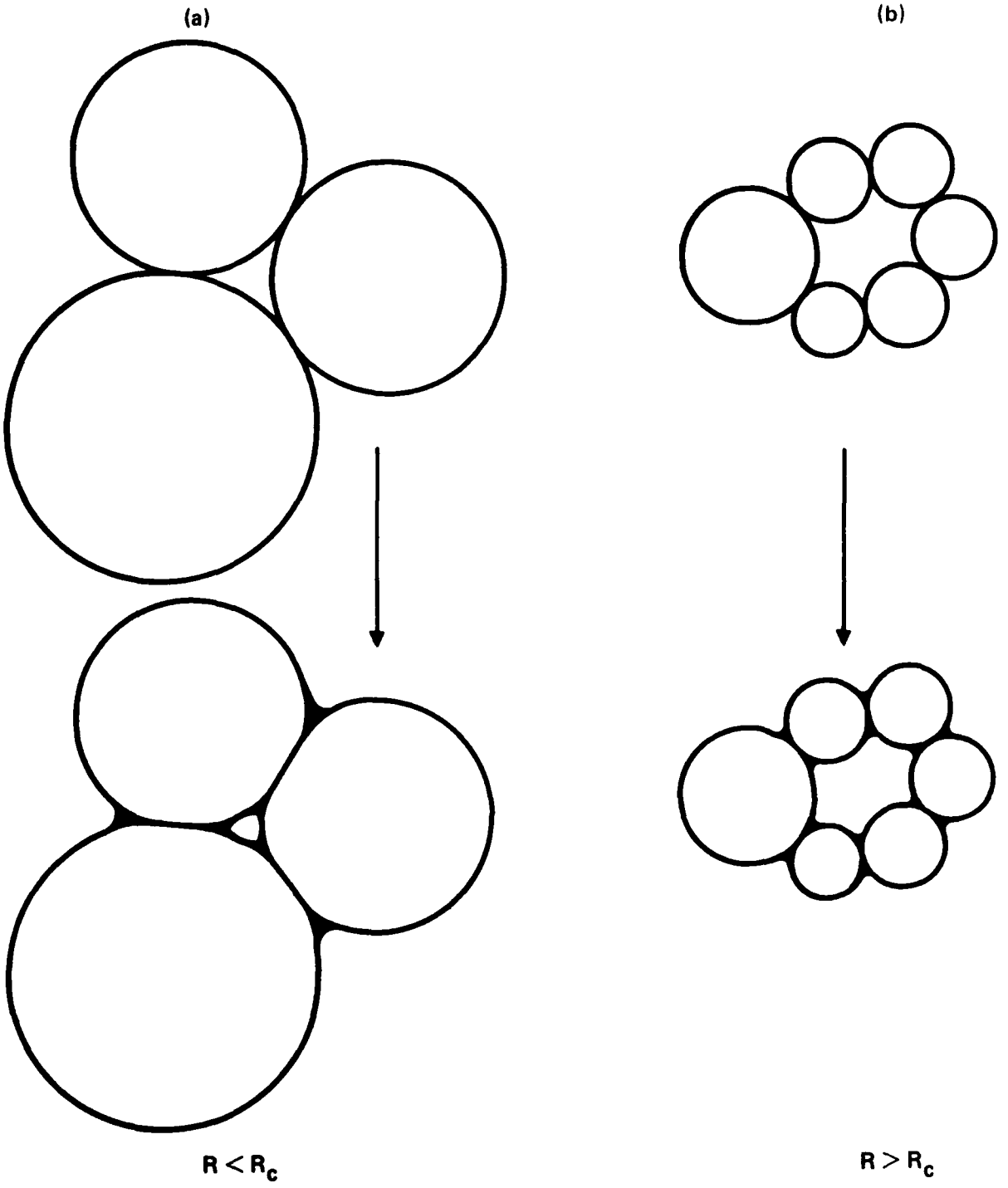

Fig. 1 Coordination number development for two pores (a) $R < R_c$ and (b) $R > R_c$.

SC83-22416

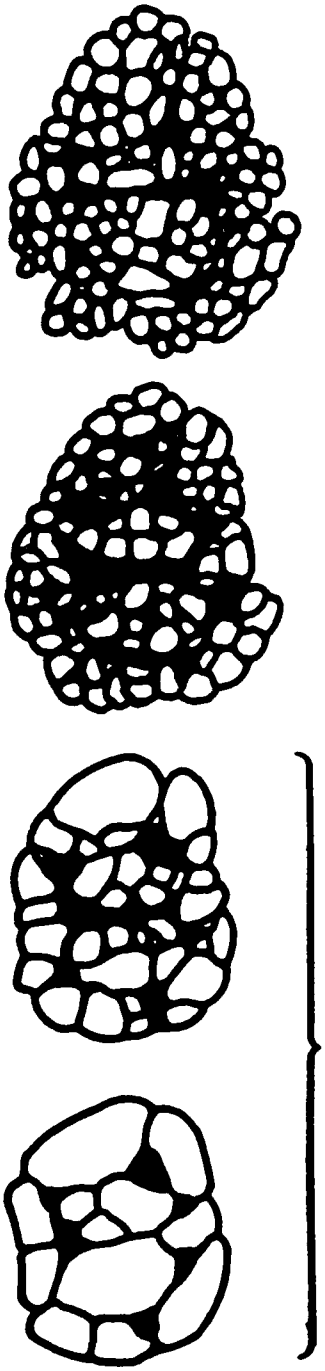

Fig. 2 Schematic for the densification of an agglomerate: local densification (or rearrangement) and grain growth.

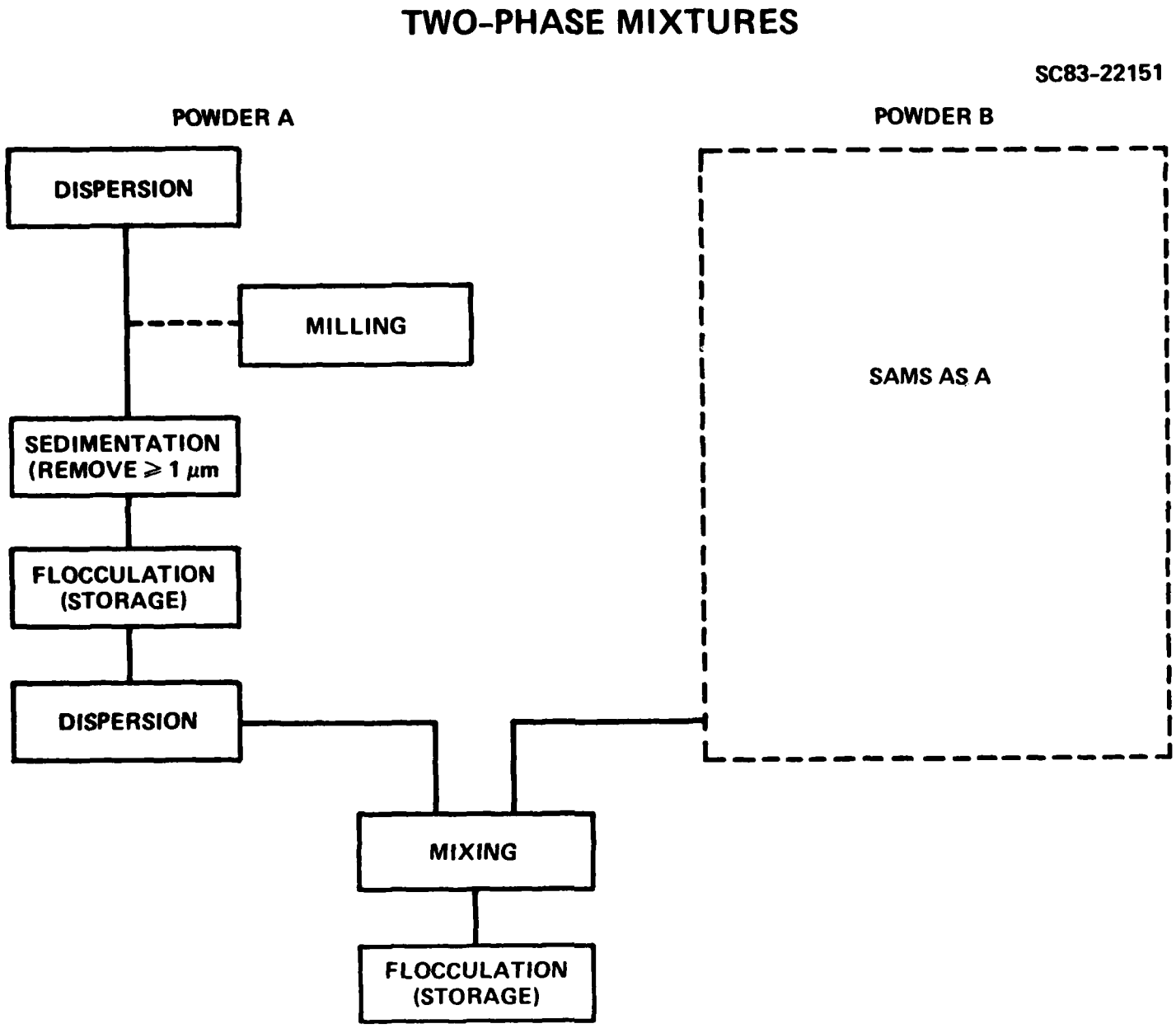

Fig. 3 Schematic for powder preparation and mixing of two phases.

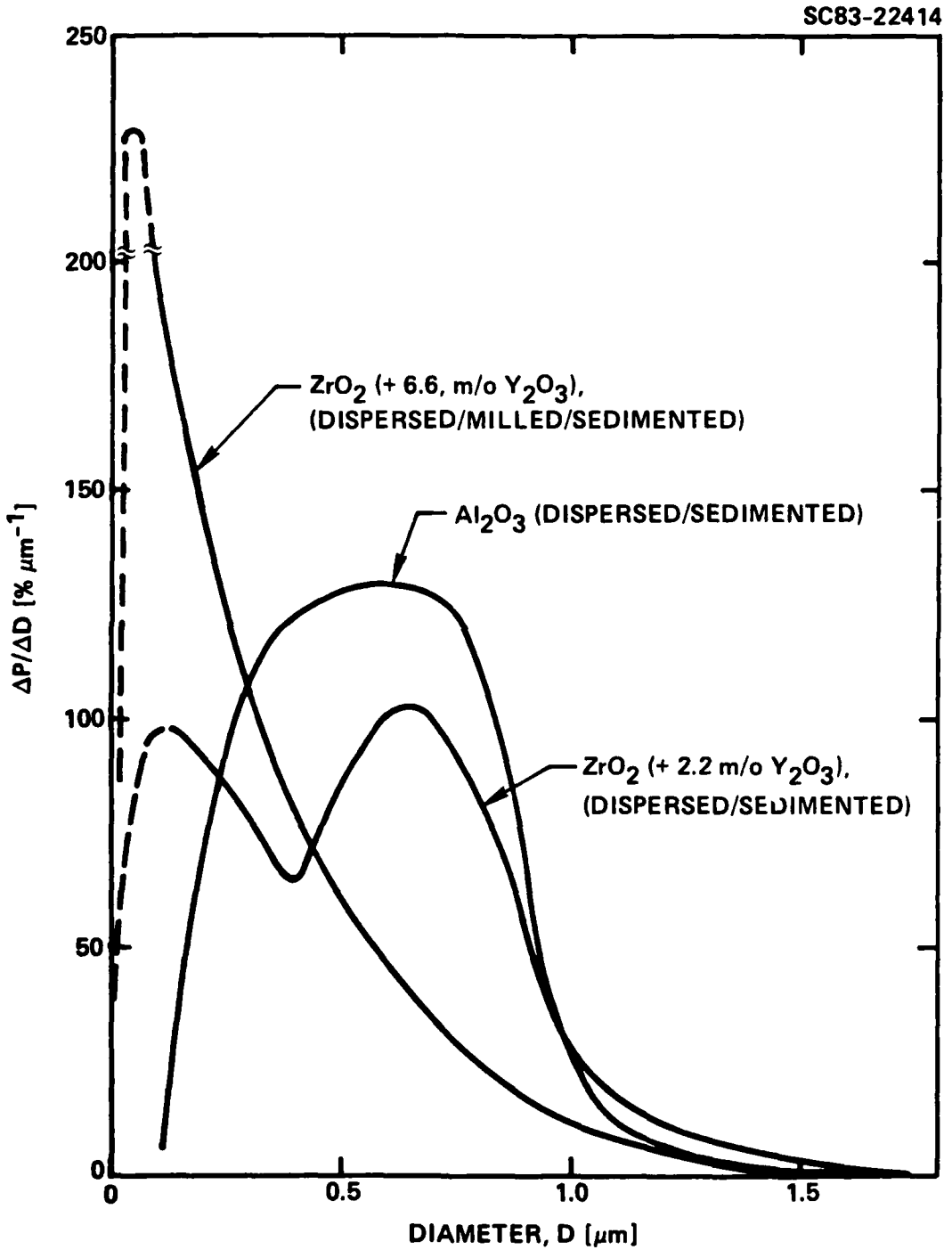

Fig. 4 Particle (or agglomerate) size distribution for three powders used in study after colloidal/sedimentation treatment.

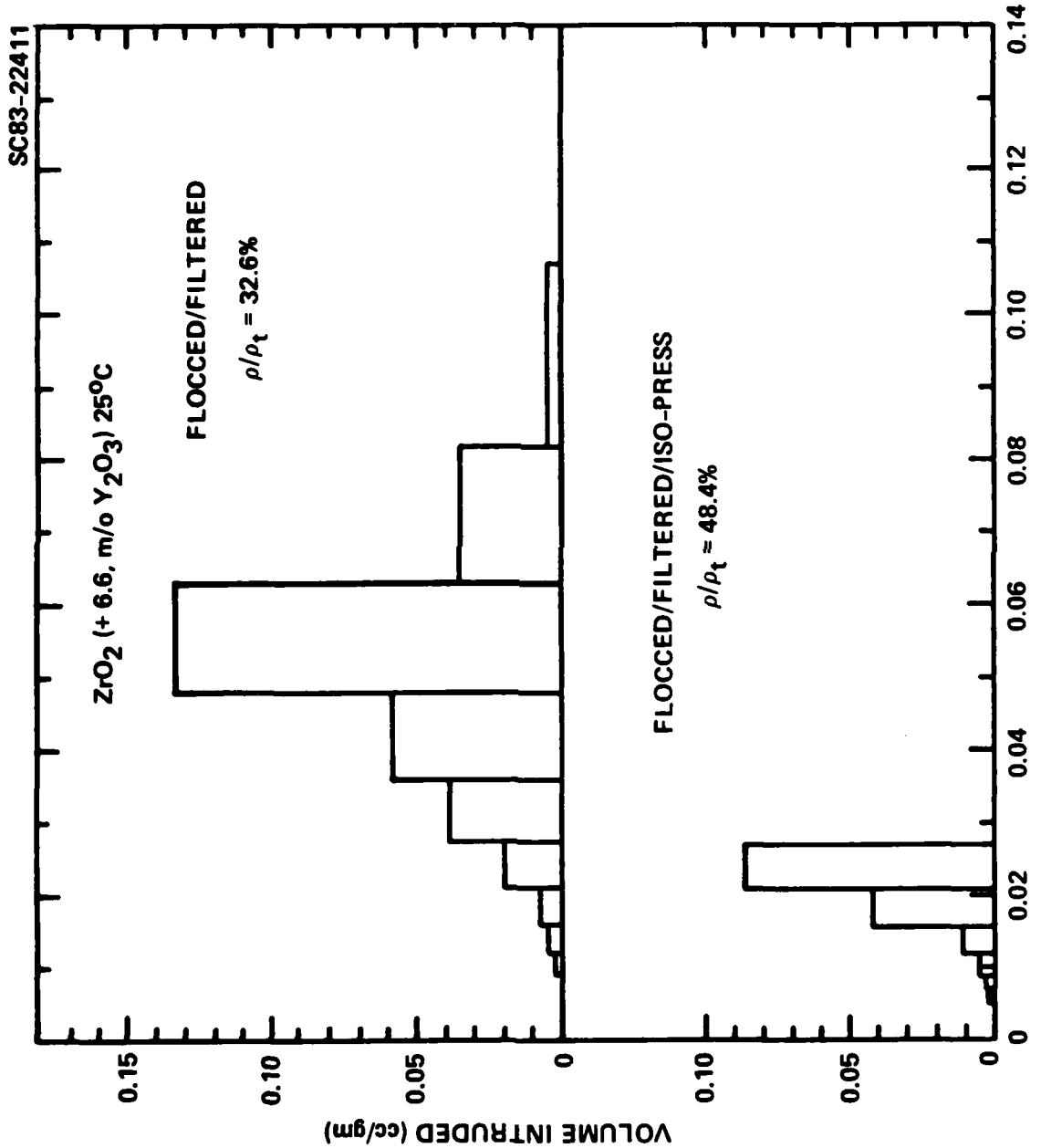

Fig. 5 Equivalent capillary size distribution (mercury intrusion) for ZrO_2 (+ 6.6 m/o Y_2O_3) compacts determined at 25°C.

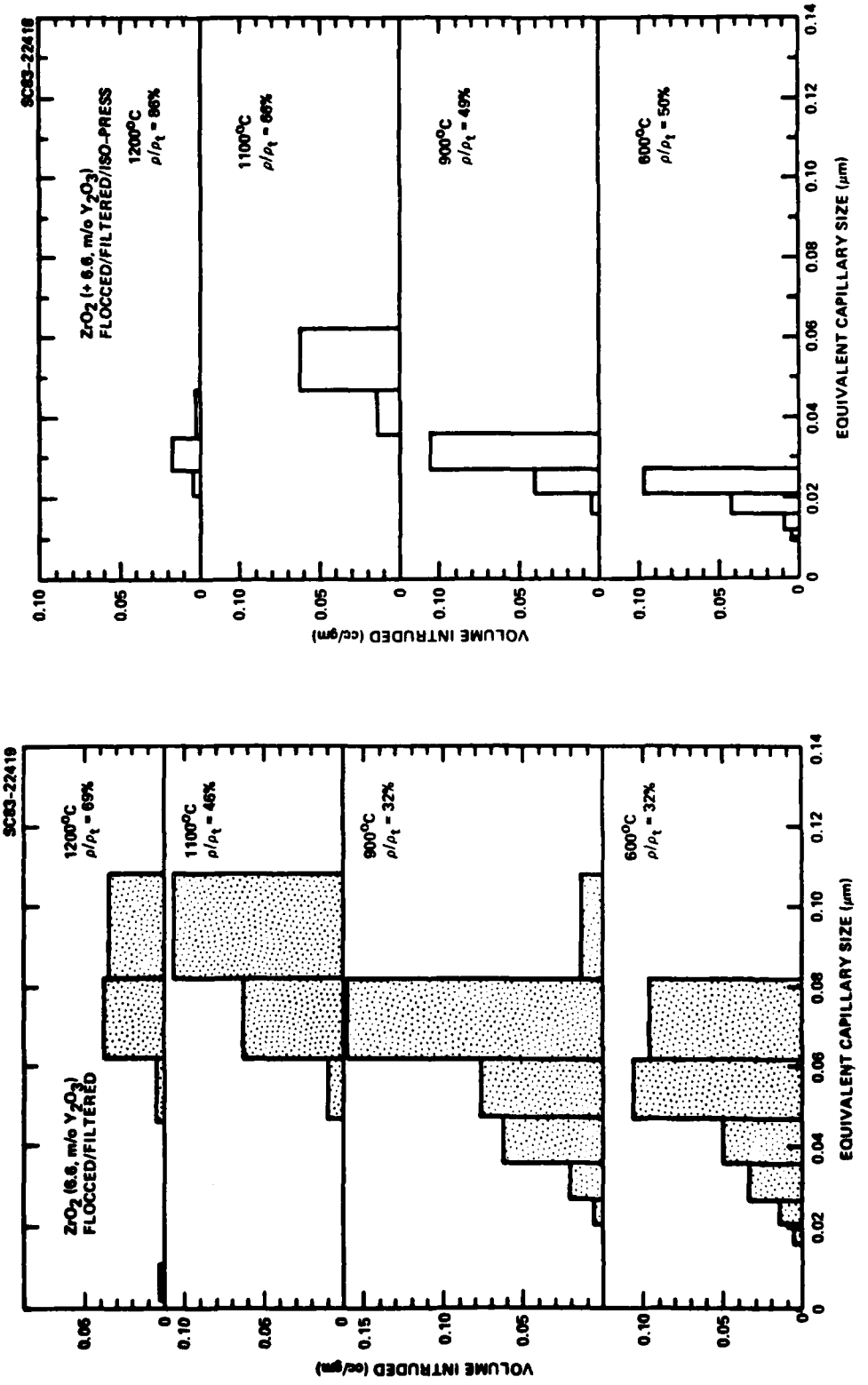

Fig. 6 Equivalent capillary size distribution (mercury intrusion) for ZrO_2 (+ 6.6 m/o Y_2O_3) as a function of temperature (30 min hold) for (a) filtered compact and (b) filtered/iso-pressed compact.

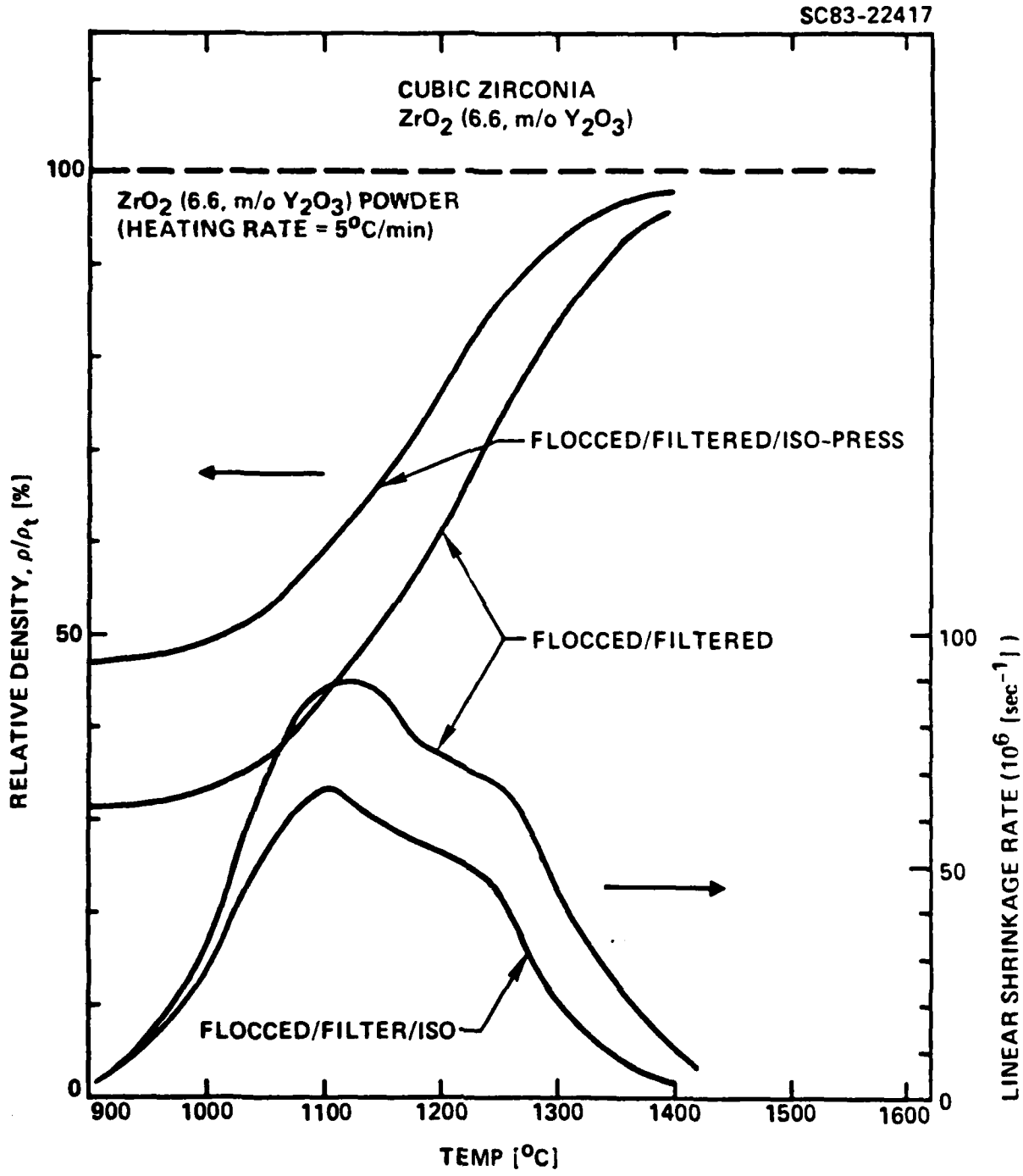

Fig. 7 Relative density and linear shrinkage rate vs temperature (heating rate = 5°C/min) for ZrO_2 (+ 6.6 m/o Y_2O_3) powder compacts (filtered and filtered/iso-pressed).

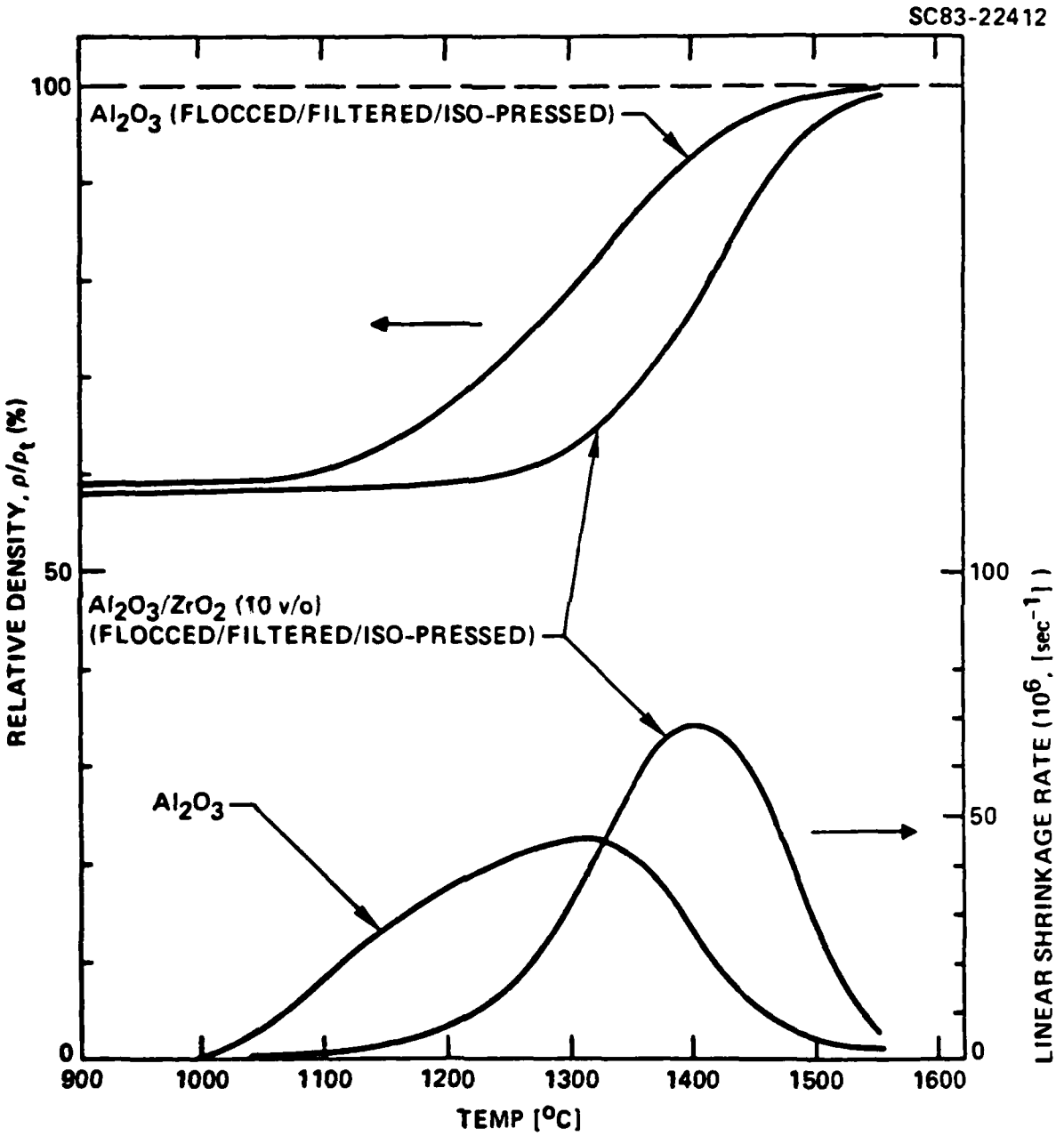

Fig. 8 Relative density and linear shrinkage rate vs temperature (heating rate = 5°C/min) for Al_2O_3 and Al_2O_3/ZrO_2 (+ 2.2 m/o Y_2O_3) powder compacts (both iso-pressed).

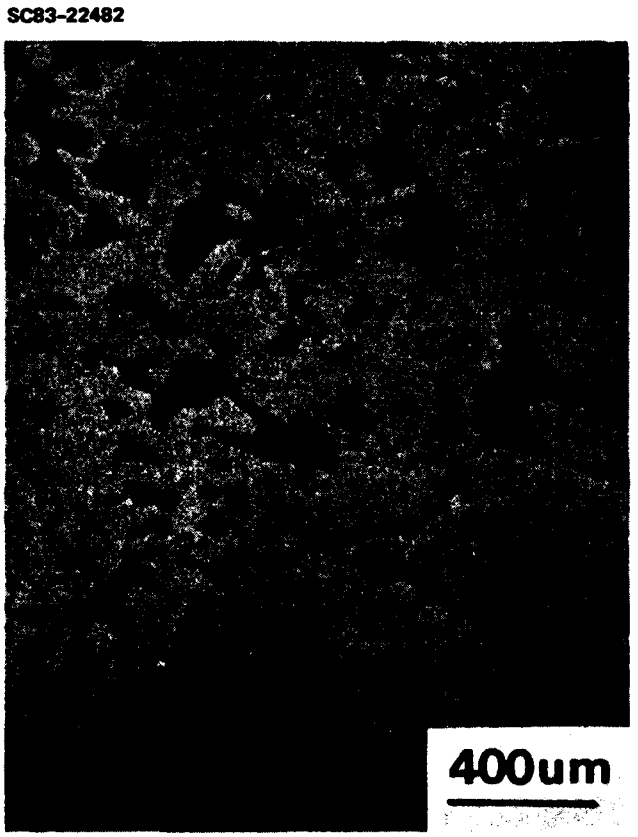

Fig. 9 Large, soft agglomerates obtained by sedimentation, packed by filtration and sintered (heating rate = $5^{o}C$/min to $1550^{o}C$. Note large pores between dense, polycrystalline domains.

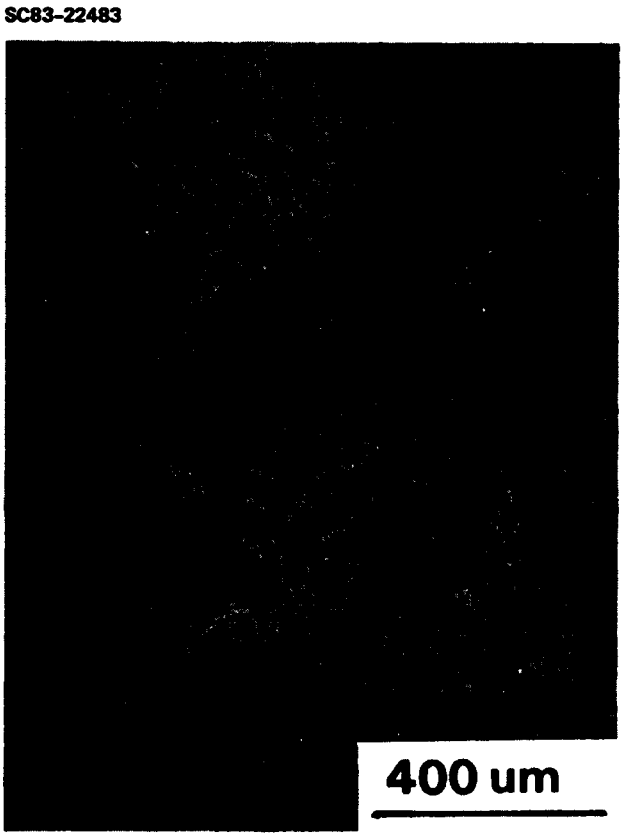

Fig. 10 Large crack-like pore produced by differential shrinkage of large Al_2O_3 agglomerate and surrounding colloidal/sedimented treated Al_2O_3 matrix (sintered 5°C/min to 1550°C).

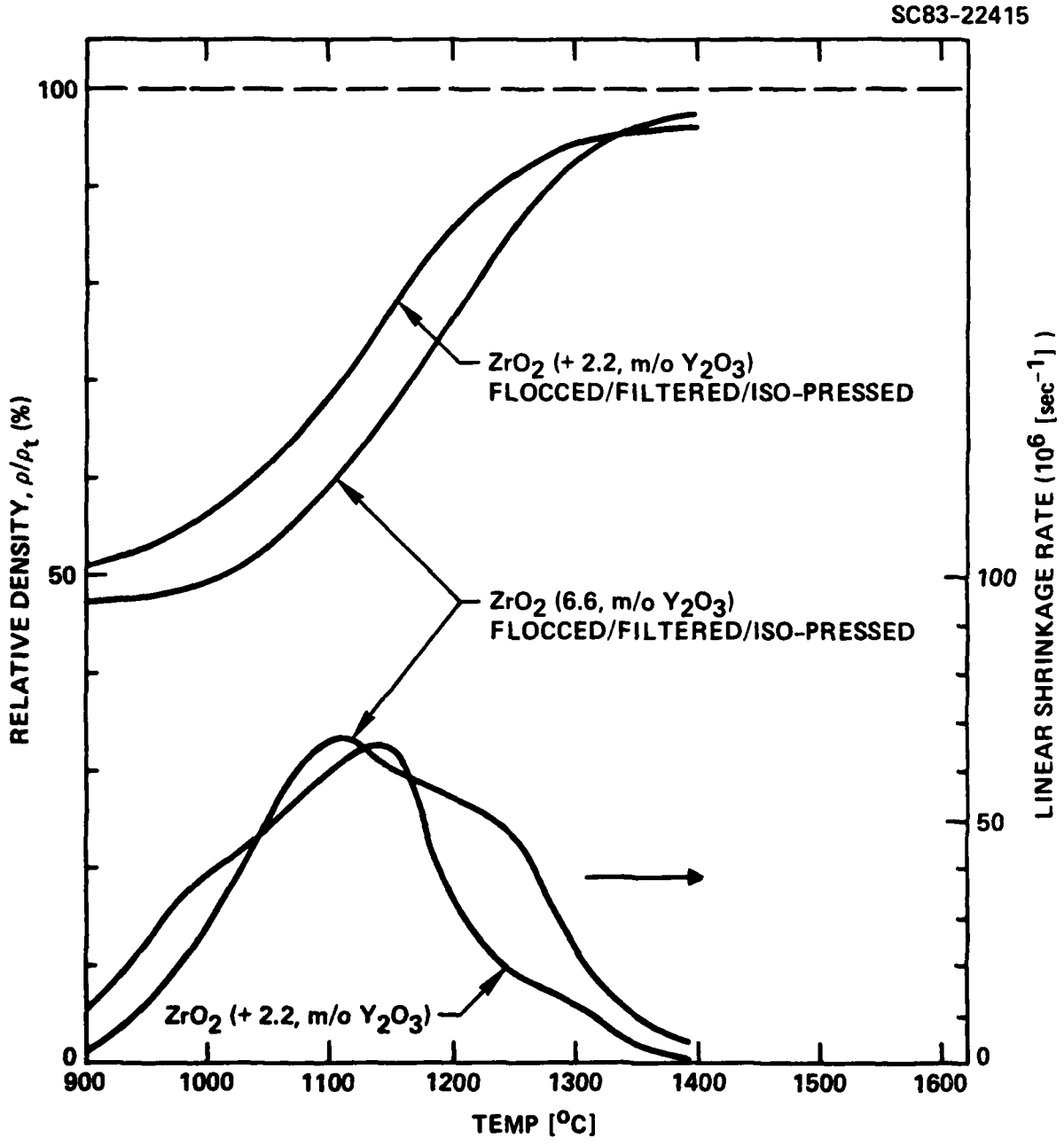

Fig. 11 Relative density and linear shrinkage rate vs temperature (heating rate = 5°C/min) for filtered/iso-pressed compacts of ZrO_2 (+2.2 m/o Y_2O_3) and ZrO_2 (+ 6.6 m/o Y_2O_3) powders.

Rockwell International
Science Center

SC5368.2FR

TECHNICAL REPORT NO. 2

(In Press: Proc. of Materials Research Soc. Conf., Boston, Nov. 1983)

SINTERABILITY OF AGGLOMERATED POWDERS

F.F. Lange
Rockwell International Science Center, Thousand Oaks, CA 91360

ABSTRACT

Powdered compacts that do not have periodic, particulate arrangements exhibit nonperiodic density variations and are, by definition, agglomerated. The void phase in the compact can be separated into pores. The pore coordination number distribution and the critical coordinated number (R_c) governs the volume fraction of pores that can spontaneously disappear by diffusion, and therefore, the compact's sinterability. The pore coordination number distribution is favorably influenced by increasing the compact's initial density and decreasing the size of the multiple particle packing unit (for example, agglomerate size). During heating the pore coordination number distribution is unfavorably shifted by local sintering, which is produced by the spontaneous disappearance of pores with favorable coordination numbers ($R < R_c$). Local densification produces a dense, polycrystalline skeletal network. Grain growth during densification, supported by dense regions, favorably alters the coordination number of pores within the skeletal network and improves sinterability. The configuration and microstructure of the dense, skeletal network will control its compliance to deformation by either effective or applied (hot pressing) compressive stresses. Deformation of the dense, skeletal network will improve the coordination number distribution and thus sinterability. From this thinking, one concludes that the ideal situation requires either a periodic particle arrangement (which requires monodispersed powders), or lacking this arrangement, alterations in surface chemistry (or structure) such that $R_c \rightarrow \infty$.

INTRODUCTION

In past decades, sintering studies have emphasized transport mechanisms and kinetics (see Ref. 1 for review). These studies suggested that the elimination of solid/vapor surface area is the driving force for densification, volume and/or grain boundary diffusion are required to produce high densities and sinterability (namely, the densification rate at a given temperature or the lowest temperature required to achieve a density close to theoretical) is inversely proportional to particle size to some power, $n > 1$. Based on this last suggestion, many investigators began to manufacture powders with very small particle sizes (so-called active powders) only to find they did not necessarily increase sinterability.

Problems associated with the sinterability of active powders are generally attributed to agglomerates, i.e., multiple particle packing units produced by either attractive (Van der Waal) interparticle forces (forming soft agglomerates which can be broken apart with surfactants) or partial sintering during calcination (forming hard agglomerates which can be broken apart by attrition). It is also generally recognized that agglomeration

alters the ideal packing arrangement of particles which, in some way, alters the sinterability from that visualized by previous theorists.*

In the past few years, investigators have started to relate the sinterability of agglomerated crystalline powders (all powder compacts which are not arranged periodically) to pore properties,** i.e., the things to be eliminated. Real packing arrangement of particles produce a variety of pore size distributions. Since smaller pores require less diffusion and should disappear first, a school [2,3] has been developing relating agglomeration to sinterability through the pore size distribution. This approach is a logical outgrowth of the classical approach, i.e., sinterability is dictated by kinetics. Although kinetics will certainly play an important role, a more recent thermodynamic approach has emphasized relations between sinterability and pore coordination number distribution. [4,5] This idea stems from theory introduced by Kingery and Francois, [6] modified by Cannon, [7] showing that pores will only disappear if their surface can develop the right type of curvature. This condition requires that the pore's coordination number, R, is less than a critical value, i.e., $R < R_c$. R_c increases with the dihedral angle (ϕ) which depends on the grain boundary (γ_{gb}) to surface energy (γ_s) ratio ($\cos(\phi/2) = \gamma_{gb}/2\gamma_s$). The larger the volume fraction of pores with $R < R_c$, the greater the sinterability. The following will emphasize how sinterability is related to pore coordination number distribution, and how this distribution is altered by powder packing procedures and heating to sintering temperatures.

PORE COORDINATION NUMBER DISTRIBUTION, V(R)

As previously detailed, [4] one can imagine particles form one or more different multiple particle packing units. For example, consider two packing units, domains and agglomerates: small groups of particles pack together to form domains, the domains pack to form agglomerates, and the agglomerates pack to form the compact. In the domains, the particle coordination is the highest, pore coordination the lowest, and the pore size the smallest. Pores between domains are larger and have a higher coordination number. Pores between agglomerates are still larger and more highly coordinated. Thus, the pore coordination number distribution will depend on the volume fraction of pores within domains, between domains, and between agglomerates as expressed by the function V(R). Thermodynamic consideration show that the volume fraction of pores that can spontaneously disappear by mass transport, kinetics permitting, is given by

$$\int_4^{R_c} V(R)\, dR \quad ,$$

where the lowest coordination number is assumed to be 4.

---

* Past theorists have generally started by examining the transport mechanisms of matter between two touching spheres, and generalized their results (or others have done it for them) to powder compacts where one assumes the powder is monodispersed spheres packed with a periodic arrangement. The lack of periodic arrangement defines a state of local density variation, and therefore, an agglomerated powder compact.

** Pores have three properties: volume (size), shape and coordination number, i.e., the number of touching particles that form the surface of the entity in the void phase of a powder compact called a pore.

CHANGES IN V(R) DURING POWDER CONSOLIDATION

Consolidation Forces

Consolidation forces either applied (e.g., isopressing) or internal (e.g., capillary forces during drying) can increase bulk density. If we assume that the consolidation forces deform the multiple particle packing units (e.g., with increasing force: agglomerates deformed by the rearrangement of domains, domains deformed by particle rearrangement, particles deformed or fractured), then it can be seen that increasing consolidation forces decreases the larger voids, that is, voids with larger coordination numbers. Namely, increasing the bulk density increases sinterability by decreasing the volume fraction of pores with $R > R_c$.

Consistent with the above arguments, experimental results show that for a given sintering condition (temperature, time) sintered density is proportional to the initial bulk density. [5,8]

Agglomerate Size

The size and coordination number of pores between the multiple particle packing units (domains and/or agglomerates) decrease with the size of the packing unit. Thus, for a fixed bulk density, sinterability should be inversely proportional to the packing unit size. Data obtained by Rhodes [9] shown in Fig. 1 for ZrO_2 agglomerated powders is consistent with this view.

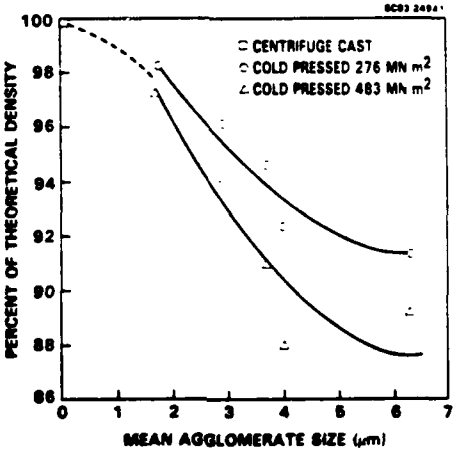

Fig. 1 Effect of agglomerate size on sintered density of ZrO_2 after 4 h at 1500°C. [9]

Powder Characteristics and Consolidation Methods

Nonagglomerated powders are desired. Hard agglomerates (partially sintered agglomerates formed during calcination, a step to be avoided) should be eliminated by innovative powder processing or controlled in size by sedimentation. Soft agglomerates can be broken apart by coloidal means, but to prevent the reformation of agglomerates, compacts must be consolidated from the particulate suspensions (dispersed or flocced). High bulk density and small agglomerate size (or floc size) should be the objective in coloidal processing.

The ideal consolidated state would be the periodic arrangement (e.g., FCC) of a monodispersed powder. In this case, the coordination number of all pores are small ($R < 6$), suggesting that most powders would be sinterable and exhibit kinetics suggested by past theory. Lacking the ability for periodic arrangement, monodispersed powders offer no particular advantage.

CHANGES IN V(R) DURING SINTERING

Local Densification

The driving force for densification can be related to an effective compressive stress (σ) given is Ref. 4:

$$\sigma = n \gamma dA' \quad , \qquad (1)$$

where n is the number of particle contacts (or necks after diffusion commences) per unit volume, γ is the surface energy per unit area and dA' is the change in the pore area per unit particle contact at a given condition (time, temperature, etc.). This relation shows that if the shrinkage rate is proportional to the driving force, multiple particle packing units with a large value of n (highly coordinated particles, pores of low coordination number) will be the first to densify.

If all packing units started to shrink at the same moment and at the same rate, then the compact would shrink uniformly. This situation could only exist for the monodispersed powder with periodic arrangement. Thus, some packing units will begin to densify earlier and/or at a faster rate than others. This leads to tensile stresses between faster densifying units relative to their surroundings: $\sigma_t = (\bar{n}-n)\gamma dA'$, where $\bar{n}$ is the average number of contacts per unit volume for the powder compact and n is that for the packing unit, $n > \bar{n}$.

These tensile stresses cause faster densifying units to break away from a portion of the surrounding matrix (break existing particle contacts and/or necks). This process, a phenomena called rearrangement by Exner [1] who attempted to explain it in a different manner, essentially transfers some void space from within the packing unit to between the packing unit and its surrounding matrix. This process increases the size and coordination number of pores between the interconnecting packing units, and thus renders the remaining pores less sinterable.

The process of local densification can be visualized as the elimination of pores with $R < R_c$ (those within the fast densifying packing units) and the increase of R for some (or all) pores with $R > R_c$.

Microstructually, local densification produces a skeletal network formed of dense interconnecting polycrystalline material and interconnecting lenticular pores.

Figure 2 shows the equivalent capillaries, determined by Hg intrusion, of a ZrO_2 powder compact heated between 600°C and 1200°C. These data show that local densification and the accompanying pore enlargement occurs prior to bulk shrinkage which initiates at 900°C. [5]

Grain Growth

As illustrated by Gupta's [10] data in Fig. 3, it has been known for many years that grain growth commences with bulk shrinkage. Recent observations show that dense regions, produced by local densification, allow and support grain growth. Pores surrounding the dense region, i.e., those en-

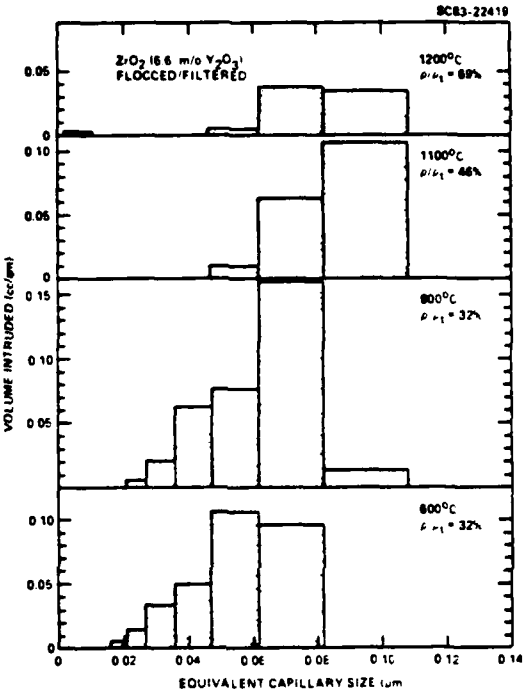

Fig. 2 Equivalent capillary size distribution, determined by Hg intrusion (for ZrO_2 + 6.6 m/o Y_2O_3) as a function of temperature (30 min hold). [5]

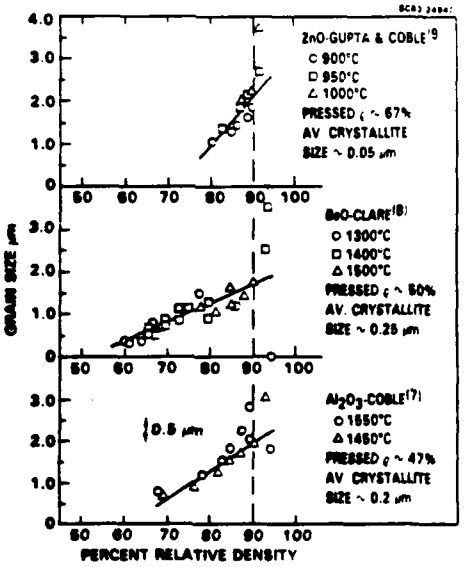

Fig. 3 Plot of density vs average grain size. [10]

larged by local densification, decrease their coordination number to become more sinterable due to the surrounding grain growth. That is, grain growth during bulk shrinkage increases sinterability* by decreasing R of the remaining pores.**

The introduction of ZrO_2 inclusions into Al_2O_3 powders are known to inhibit grain growth. [11] These inclusions also delay sinterability by ~ 100°C [12] as shown in Fig. 4.

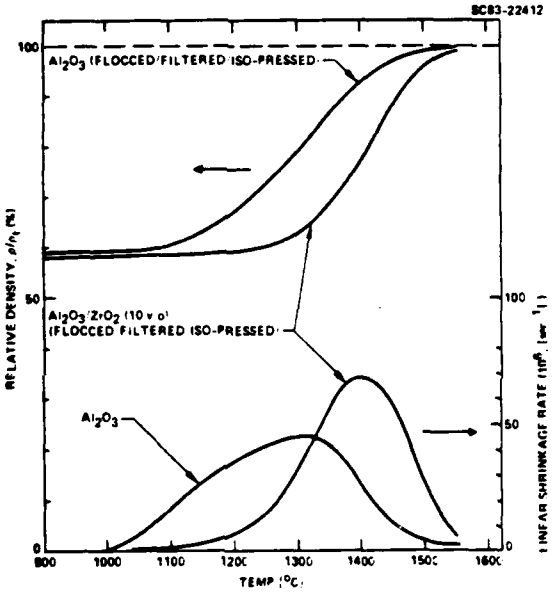

Fig. 4 Relative density and linear shrinkage rate vs temperature for Al_2O_3 and Al_2O_3 (+ 2.2 m/o Y_2O_3) powder compacts. [5]

Creep

Recognizing now that the microstructure of a densifying powder compact is not represented by connecting particles with necks in various stages of growth, but by the skeletal network of interconnecting dense, polycrystalline regions and interconnecting lenticular porosity, the role of stresses (e.g., hot-pressing) takes on new meaning. Conventional thinking suggests that applied stresses, acting on contact regions between particles, added to the chemical potential difference that existed at different pore surface locations and, thus, enhanced the driving force for diffusivity and pore disappearance. Although the importance of this phenomena cannot be refuted, a major role of the applied stresses* is to deform the dense, skeletal network to either close or partially close the lenticular shaped pores. Partial

* Abnormal grain growth during latter stages with smaller pores should still be discouraged.
** Grain growth does not necessarily decrease pore size.
† Or, the effective compressive stress exerted by the surface area change (see Eq. (1)).

closure of some pores will reduce their coordination number to $R < R_c$ so that they can spontaneously disappear by sintering. The configuration of the skeletal network and its polycrystalline microstructure are expected to play an important role in governing its compliance to creep.

SUMMARY

Previous thinking concerning sintering neglected effects due to particle arrangement, which can dominate sinterability. Agglomerates are known to limit sinterability and to produce a nonuniform particle arrangement. Current thinking directing relationships between agglomeration and sintering are concerned with the size and coordination number of the pores produced by the nonuniform particle arrangement.

The purpose of this review was to show that although pore size may determine sintering kinetics, it is the pores coordination number which governs whether or not it can disappear, i.e., only pores coordinated by less than a certain number of particles (or grains) can disappear. The concept that the pore coordination number distribution is the most important property of the powder compact relative to the pore size distribution is based on the fact that the thermodynamics must be satisfied first before one discusses kinetics. The effect of initial bulk density and agglomerate (or multi-particle packing units) size on the compacts sinterability can be explained with either the kinetics (pore size distribution) or the thermodynamic (pore coordination number distribution) viewpoint. On the other hand, local densification and the effect of grain growth on sinterability can best be explained with the thermodynamic viewpoint. In either case, people today are attempting to explain sinterability in terms of pore properties, i.e., in terms of things we want to disappear. In general, the thermodynamic approach suggests that the ideal conditions for sinterability are periodic particle arrangements and/or chemical surface states that cause $R_c \to \infty$ (i.e., $\phi \to 180°$).

ACKNOWLEDGEMENTS

This review was written under Rockwell financial support (IR&D funds) at Chalmers University, Goteburg, Sweden.

REFERENCES

1. H.E. Exner, "Principles of Single Phase Sintering," Reviews on Powder Metallurgy and Physical Ceramics 1, (1-4), T.1-251 (1979).
2. K. Haberko, "Characteristics and Sintering Behavior of ZrO_2 Ultrafine Powders," Ceramics Int'l. 5, 148 (1979).
3. A. Roosen and H. Hausner, "Sintering Kinetics of ZrO_2 Powders," Proc. ZrO_2 Conf., Stuttgart, June 1983.
4. F.F. Lange, "Sinterability of Agglomerated Ceramic Powders," submitted to J. Ceram. Soc.
5. F.F. Lange and B.I. Davis, "Sinterability of ZrO_2 and Al_2O_3 Powders: The Role of Pore Coordination Number Distribution," Ibid, Ref. 3.
6. W.D. Kingery and B. Francois, "Sintering of Crystalline Oxides, I: Interaction Between Grain Boundaries and Pores," in Sintering and Related Phenomena, eds., G.C. Kuzynske, N.A. Hooten and G.F. Gibbon, pp. 471-98, Gordon Breach, 1967.
7. R.M. Cannon, "The Effect of Dihedral Angle and Pressure on the Driving Forces for Pore Growth and Shrinkage," to be published.
8. T. Vasilos and W. Rhodes, "Fine Particulates to Ultrafine/Grain Ceramics," in Ultrafine Grain Ceramics, eds. J.J. Durke, N.L. Reed and V. Weiss, pp. 137-172, Syracuse Univ. Press, 1970.

9. W.H. Rhodes, "Agglomerate and Particle Size Effects on Sintering Yttria-Stabilized Zirconia," J. Amer. Ceram. Soc. 64, 19 (1981).
10. T.K. Gupta, "Possible Correlations Between Density and Grain Size During Sintering," J. Amer. Ceram. Soc. 55 (5), 276 (1972).
11. F.F. Lange and M. Hirlinger, "Effect of ZrO_2 Dispersion on the Grain Growth of Al_2O_3," submitted to Amer. Ceram. Soc.
12. F.F. Lange, T. Yamaguchi and P.E.D. Morgan, "Effect of ZrO_2 Dispersion on the Sintering of Al_2O_3," to be published.

Rockwell International
Science Center

SC5368.2FR

TECHNICAL REPORT NO. 3

EFFECT OF ZrO_2 INCLUSIONS ON THE SINTERABILITY OF Al_2O_3

F. F. Lange, Takashi Yamaguchi,*
B. I. Davis and P. E. D. Morgan
Structural Ceramics
Rockwell International Science Center
Thousand Oaks, California 91360

*While on sabbatical from Keio University, Japan.

ABSTRACT

The sinterability of Al_2O_3/ZrO_2 composite powder compacts containing 2 v/o and 10 v/o ZrO_2 were compared to the sinterability of their single-phase constituents through constant heating rate experiments. The ZrO_2 inclusion phase delayed the initiation of bulk shrinkage and the temperature of maximum strain rate by ~ 100°C. The ZrO_2 inclusion phase also significantly inhibited grain growth. These results are discussed with regard to the thermodynamics of pore disappearance which suggests that grain growth during most stages of sintering is desirable since it decreases the coordination number of pores. Thus phenomena that inhibit grain growth are expected to inhibit densification.

1.0 INTRODUCTION

In a previous paper,[1] it was suggested that grain growth during sintering was advantageous to densification. This reasoning was developed by recognizing that pores within a partially sintered powder compact only shrink to an equilibrium size unless the number of grains coordinating the pore is less than a critical number (N_c). As introduced by Kingery and Francois,[2] the number of coordinating grains (N) and the dihedral angle (ψ, which is governed by the ratio of the grain boundary to surface energies) dictate the pore's surface curvature and therefore its thermodynamic ability to disappear. Looking from within the pore, concave surfaces are required to cause mass transport to fill the pore and make it disappear.* As illustrated in Fig. 1, grain growth can reduce the pore coordination number from $N > N_c$ (the case where the pore has a metastable size) to $N < N_c$ (the case where the pore can spontaneously disappear).

Since grain growth is known to occur throughout all stages of sintering,[3] it was hypothesized that grain growth is helpful in densification by reducing the coordination number of unfavorably coordinated pores. Different experiments were initiated to test this hypothesis. The experiments reported here are concerned with the sinterability of Al_2O_3 and two-phase Al_2O_3/ZrO_2 powders. Previous studies[4] have shown that ZrO_2 grains hinder the growth of Al_2O_3 grains in fully dense materials. It was thus the object of this work to determine if ZrO_2 would also hinder the sinterability of Al_2O_3.

*Long range diffusion between surfaces of different convex curvatures (e.g., different pores) which may not lead to shrinkage, is neglected here.

2.0 BACKGROUND

A previous study[3] has shown that grain growth in dense Al_2O_3/ZrO_2 (0 to 0.10 volume fractions) composites is inhibited by the ZrO_2 inclusion phase. The composites were prepared by mixing aqueous dispersion Al_2O_3 and ZrO_2 powders prior to consolidation and sintering. The mean size of the ZrO_2 particles were ~ 0.1 that of the Al_2O_3 particles. They became located at energetically favorable 4-grain, Al_2O_3 junctions during densification. The inclusions exerted a dragging force at the 4-grain junction to limit normal growth of the Al_2O_3 grains by 15% to 50% depending on the post-sintering heat treatment temperature. Growth of the ZrO_2 inclusions occurred by coalescence. Abnormal grain growth occurred when the ZrO_2 inclusions were poorly distributed (low volume fractions) and did not uniformally inhibit the growth of all Al_2O_3 grains.

Dihedral angle measurements of ZrO_2 grains, symmetrically located on Al_2O_3 grain boundaries, indicated tha the Al_2O_3/ZrO_2 interfacial energy is ≈ 2/3 the average Al_2O_3 grain boundary energy. This result would tend to suggest that if the difference between surface and grain boundary (or interfacial) energies was the only factor influencing sinterability, the Al_2O_3/ZrO_2 composite powders should be more sinterable relative to the single phase Al_2O_3 powders. In addition, although a third phase is not produced in the Al_2O_3 + ZrO_2 reaction, Al^{+3} is slightly soluable[5,6] in ZrO_2 suggesting that diffusivity and sinterability might be enhanced by defects created by this slight solid solubility. Based on these observations and conversional thinking, one might conclude that ZrO_2 inclusions might increase the sinterability of Al_2O_3.

3.0 EXPERIMENTAL PROCEDURE

Single-phase Al_2O_3,* ZrO_2 and two series of Al_2O_3/ZrO_2 composite powders containing 2 v/o and 10 v/o ZrO_2 were prepared for sintering studies. Two different ZrO_2* powders were used. One (c-ZrO_2)** contained 6.6 mole % Y_2O_3 in solid solution and had a cubic structure. The second (TWCA-ZrO_2)*** did not contain a solid solution additive and was amorphous when examined by x-ray diffraction analysis.

The Al_2O_3§ and c-ZrO_2 powders were separately prepared for consolidation with a procedure outlined in Fig. 2. This procedure consisted of dispersing the powder in water with sufficient HCl to maintain a pH of 2, sedimentering to remove hard agglomerates and particles $\gtrsim$ 1 μm, and flocculating the retained dispersion with NH_4OH. Flocculating increased the volume fraction of the powder and prevented mass segregation during storage. The flocced slurry was washed three times to remove excess salts by removing the clear supernate, adding deionized water, and reflocculating without additions of either acid or base.

The TWCA-ZrO_2 powder was shipped as an aqueous slurry at pH = 1.8. No sedimented layer was observed on the bottom of the containers after a period of ~ one month. The dispersion was prepared by simply flocculating with NH_4OH and washing as indicated above.

The two series of Al_2O_3/ZrO_2 composites containing 2 v/o and 10 v/o ZrO_2 were prepared by first redispersing the flocced single-phase slurries, measuring their densities to determine the solid volume content and then

* Sumotomo Chemical Co., Japan (AKP-30 Al_2O_3).
** Zircar, Florida, N.Y.
***Teledyn-Wah Chang Albany. Pregpm 97321.
§ The Sumitomo Al_2O_3 powder has corundum structure; particles have a roundish morphology. The manufacturer claims total cation impurities of < 50 ppm. The powder did not appear to contain any hard (partically sintered) agglomerates but did contain large soft agglomerates which could be broken apart during dispersion with the aid of an ultrasonic horn.

mixing the appropriate weight factions of each dispersed phase together with the aid of an ultrasonic horn. The mixing of two compatible dispersed phases is analogous to the mixing of two rare gases. Once mixed, the two-phase dispersions were immediately flocced to prevent mass segregation and to preserve the uniform phase distribution of the dispersed state.

All flocced slurries were consolidated by filtering (slip cast) in cylinderical teflon molds on casting plaster. After drying, the cylindrical powder compacts were iso-pressed at 350 MPa. Iso-pressing helped to insure that the relative bulk densities of the Al_2O_3 and Al_2O_3/ZrO_2 powder compacts were nearly identical prior to sintering.

Several Al_2O_3/ZrO_2 composite specimens were also prepared by mixing the dry, untreated Al_2O_3 powder into water at pH 2 and then mixing with the appropriate amount of the treated ZrO_2 dispersion as described above. This procedure did not break apart all of the Al_2O_3 soft agglomerates, resulting in single-phase Al_2O_3 regions within the well mixed, two-phase material. These specimens, were used to illustrate the effect of the ZrO_2 on inhibiting grain growth.

Sintering studies were carried out in a programmed furnace that could maintain a constant heating rate of up to 20°C/min to 1600°C. A high temperature extensometer described elsewhere,[7] was used to measure linear shrinkage that occurred during the constant heating rate sintering experiments. For each experiment, the temperature was raised at 5°C/min to 1550°C (1400°C for the two ZrO_2 powders.) Extensometer strain was recorded vs temperature over the entire heating period. Final sintered density, determined by Archeridies method, and initial bulk density were compared with the total recorded strain to insure accuracy in the linear shrinkage measurements. After entering the data into a computer, density was calculated as a function of temperature (ρ_T) using $\rho_T = \rho_0 (1-\varepsilon)^{-3}$, where ρ_0 = initial bulk density and ε = strain at desired temperature. Strain rate ($\dot{\varepsilon}$) were also determined as a function of temperature.

4.0 RESULTS

4.1 Single-Phase Material

Figure 3 illustrates the size distribution of the colloidally treated Al_2O_3 and c-ZrO_2 powders. Since the instrument used to determine size distribution is not effective below ~ 0.1 μm, the broken line for c-ZrO_2 only indicates that many particles are < 0.1 μm. For the same reason, attempts to measure the size distribution of the TWCA-ZrO_2 powder indicated that all particles were < 0.1 μm. As indicated by its manufacturer, the size distribution of the Al_2O_3 powder was narrow relative to other Al_2O_3 powders previously examined.

Figure 4 illustrates the density (a) and strain rate data (b) vs temperature (heating rate of 5°C/min) and Table I reports the initial relative bulk density, the relative density after the constant heating rate experiment, and the temperature at which the strain rate reached a maximum value.

4.2 Two-Phase Materials

The density and strain rate data for all four two-phase materials were nearly identical. Figure 5 illustrates the comparison of these data with the single-phase Al_2O_3 data. Table I reports other pertinent data. It should be noted that bulk densification and the maximum strain rate are both delayed by ~ 100°C with additions of either 2 v/o or 10 v/o ZrO_2 to the Al_2O_3.

4.3 Microstructures

Figure 6 illustrates a backscatter SEM micrograph typical of the poorly mixed Al_2O_3/ZrO_2 composites consolidated during initial study period. These specimens were sintered at 1550°C/3 hrs, polished, and thermally etched at 1450°C/1 hr. The apparent porosity in the two-phase regions was produced by ZrO_2 pullouts during polishing. The darker phase is Al_2O_3. The large single-phase region is a remnant of the poorly mixed, Al_2O_3 soft agglomerate. This micrograph clearly illustrates the effect of the ZrO_2

inclusion phase on limiting the grain growth of the high purity* Al_2O_3 powder used in this study.

5.0 DISCUSSION

This study clearly illustrates that the two-phase Al_2O_3/ZrO_2 powder compacts require a higher sintering temperature to achieve a comparable density relative to their constituents. Of greater interest here, if one were to accept the thermodynamic arguments concerning pore disappearance, is the fact that the ZrO_2 inclusions both inhibit the grain growth and the sinterability of Al_2O_3. This thermodynamic argument suggests that one must reduce the coordination number of pores. Grain growth is one phenomenon which would reduce the coordination number, viz, grain growth during most stages of sintering is desirable. Thus, inhibiting grain growth would inhibit densification.

No doubt other agreements, concerned with either chemical or particle arrangement effects, might be put forth to explain the inhibiting effect of ZrO_2 on the sinterability of Al_2O_3. Two chemical effects, viz, one concerned with changes in sintered surface enbergies, and the other concerned with defect enhanced diffusion, were discussed in a previous section. Particle arrangement also influences sinterability. In the extreme, the ZrO_2 inclusions could be considered as inert to simply decrease the effective initial bulk density of the Al_2O_3 powder compact. As reported elsewhere,[8] a 7% decrease in the bulk density of the same Al_2O_3 used here (not iso-pressed) does increase the temperature where the strain rate reaches a maximum from 1310°C to 1330°C, but unlike the data reported in Fig. 4, for the Al_2O_3/ZrO_2 composites, the temperature where shrinkage initiates remains unchanged. Also, if the effect of the ZrO_2 were to decrease bulk density, one would expect differences in the densification data for composites containing 2 v/o and 10 v/o ZrO_2 inclusions. Such differences were not observed.

Thus, based on thermodynamic analysis and experimental result, it can

*Previous grain growth studies[4] were carried out with a less pure Al_2O_3 powder.

be consistently argued that grain growth during most stages of sintering* is desirable and phenomena that inhibit grain growth will inhibit sinterability.

6.0 REFERENCES

1. F. F. Lange, "Sinterability of Agglomerated Powders," J. Am. Ceram. Soc. 67[2], 83-9 (1984).

2. W. D. Kingery and B. Francois, "Sintering of Crystalline Oxides, I. Interaction Between Grain Boundaries and Pores," pp. 471-98 in sintering and Related Phonema. Edited by G. C. Kuczynke, N. A. Hooton, and G. F. Gibbon, Gordon Breach, New York (1967).

3. T. K. Gupta, "Possible Correlations Between Density and Grain Size During Sintering," J. Am. Ceram. Soc. 55[5], 176-77 (1972).

4. F. F. Lange and Margaret M. Hirlinger, "Hindrance of Grain Growth in Al_2O_3 by ZrO_2 Inclusions," J. Am. Ceram. Soc. 67[3] 164-8 (1984).

5. D. R. Clarke, private communication.

6. F. L. Lange, H. Shubert, M. Ruhler and N. Claussen, "Effect of Attrition Milling and Post-Sintering Heat Treatment on Fabrication, Microstructure anf Properties of Transformation Toughened ZrO_2," to be published.

7. F. F. Lange, B. I. Davis and D. R. Clarke, "Compressive Creep of Si_3N_4 MgO Ceramics: Part 1 Effect of Compositions," J. Mat. Sci. 15 601-10 (1980).

8. F. F. Lange and B. I. Davis, "Relations Between Shrinkage Strain, Strain Rate and Rearrangements During Sintering: Experimental Observations with Al_2O_3, ZrO_2 and Al_2O_3/ZrO_2 Powder Compacts," to be published.

ACKNOWLEDGEMENTS

This work was performed for the Office of Naval Research, Contract No. N00014-83-C-0469.

*Abnormal grain growth during the last stage of densification, which traps pores within grains is still undesirable.

Table I

Sintering Data for Single- and Two-Phase Materials

Material	Initial Relative Bulk Density	Final Relative Density	Theoretical Density ($gm\text{-}cm^{-3}$)	Temperature of Maximum $\dot{\varepsilon}$ (°C)
Al_2O_3	0.59	0.99	3.98	1310
c-ZrO_2	0.47	0.97	6.05	1100
TWCA-ZrO_2*	0.44	0.99+	5.85	1145
Al_2O_3/c-ZrO_2(2 v/o)	0.59	0.99	4.02	1400
Al_2O_3/c-ZrO_2 (10 v/o)	0.58	0.99	4.19	1400
Al_2O_3/TWCA-ZrO_2 (2 v/o)**	0.59	0.99	4.02	1400
Al_2O_3/TWCA-ZrO_2 10 v/o)**	0.57	0.99	4.19	1410

* Sintered material is monoclinic ZrO_2.
** Tetragonal ZrO_2 constrained by Al_2O_3.

SC84-27084

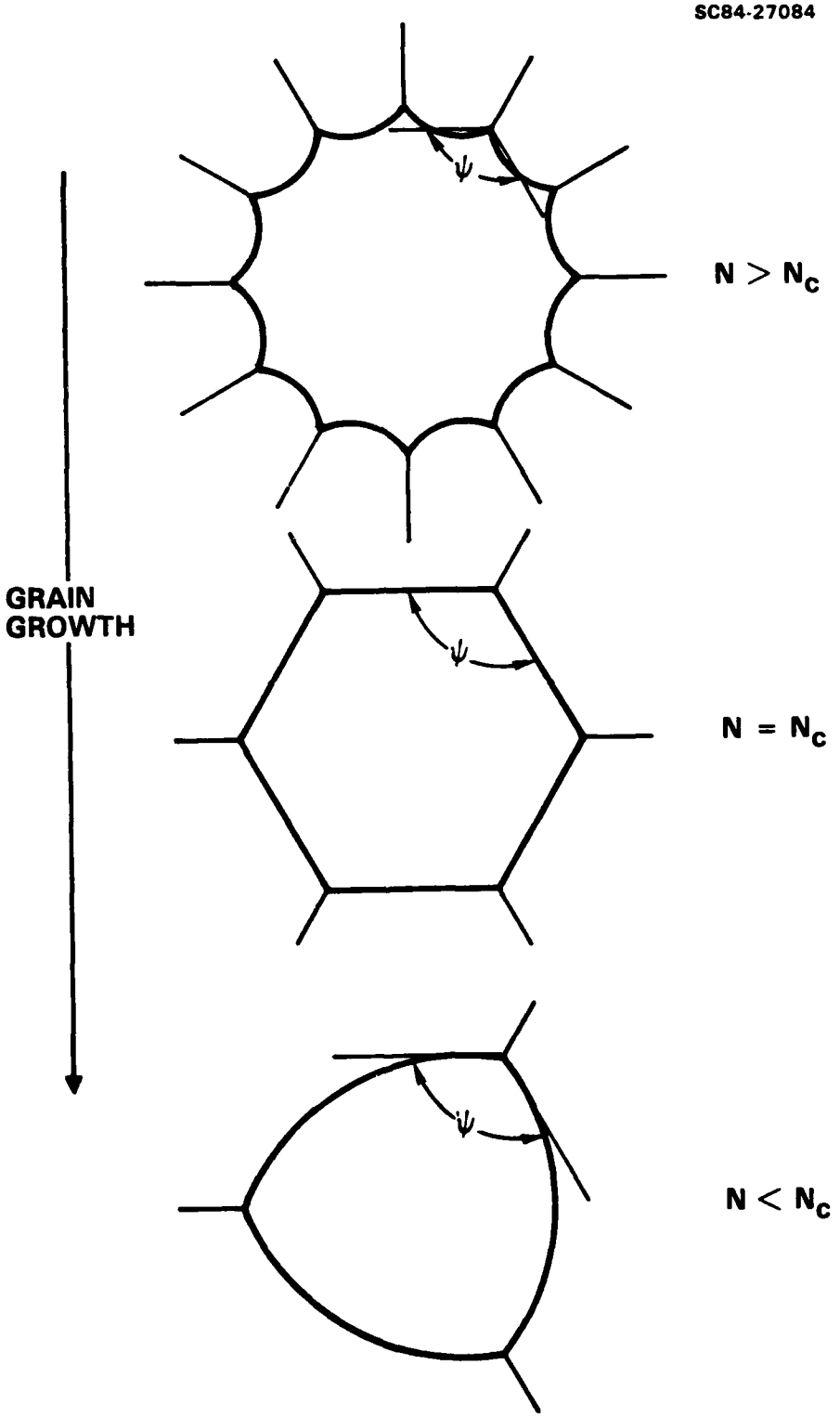

Fig. 1 Schematic of change in pore coordination number (N) with grain growth.

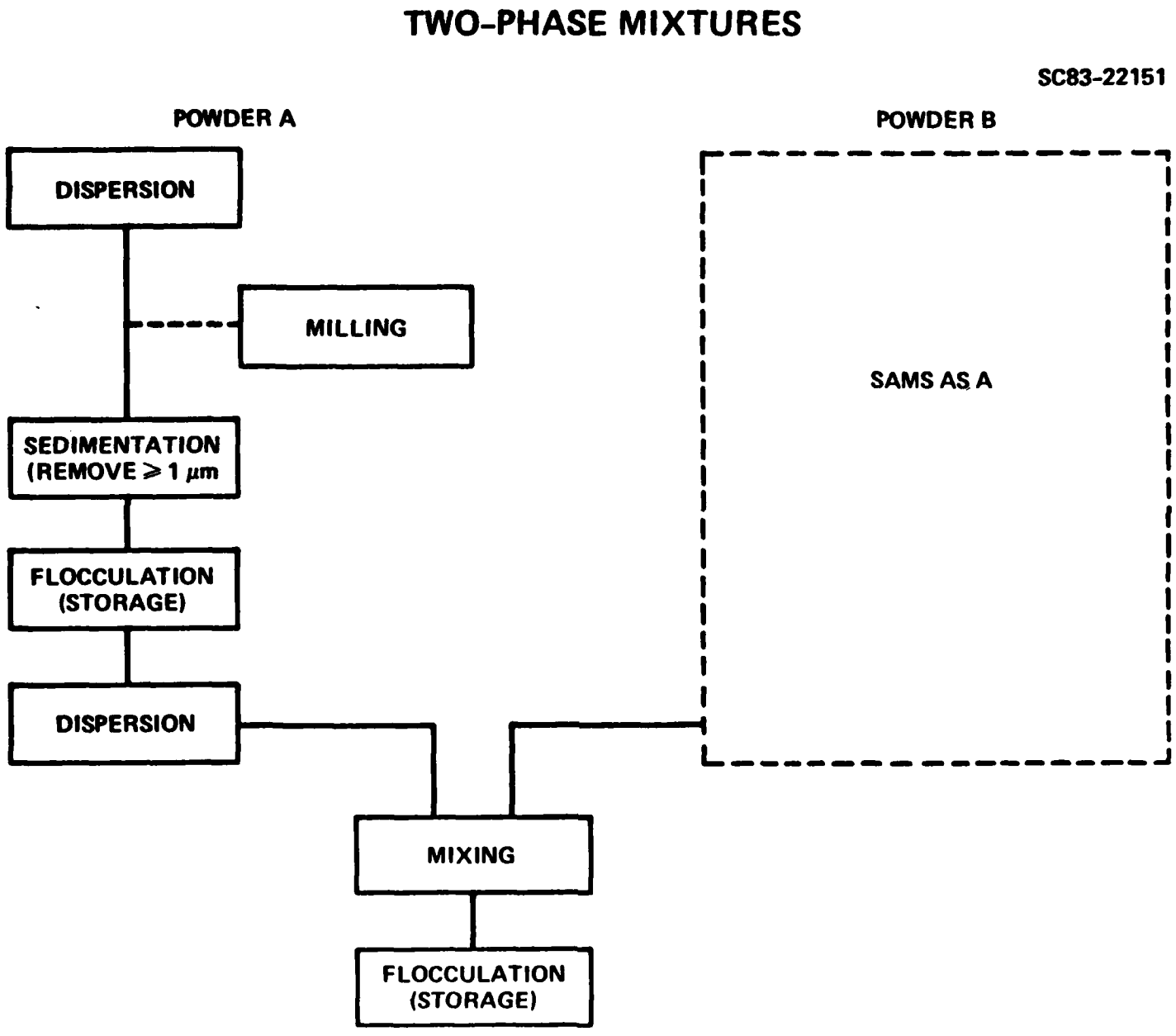

Fig. 2 Schematic of colloidal method of processing powders.

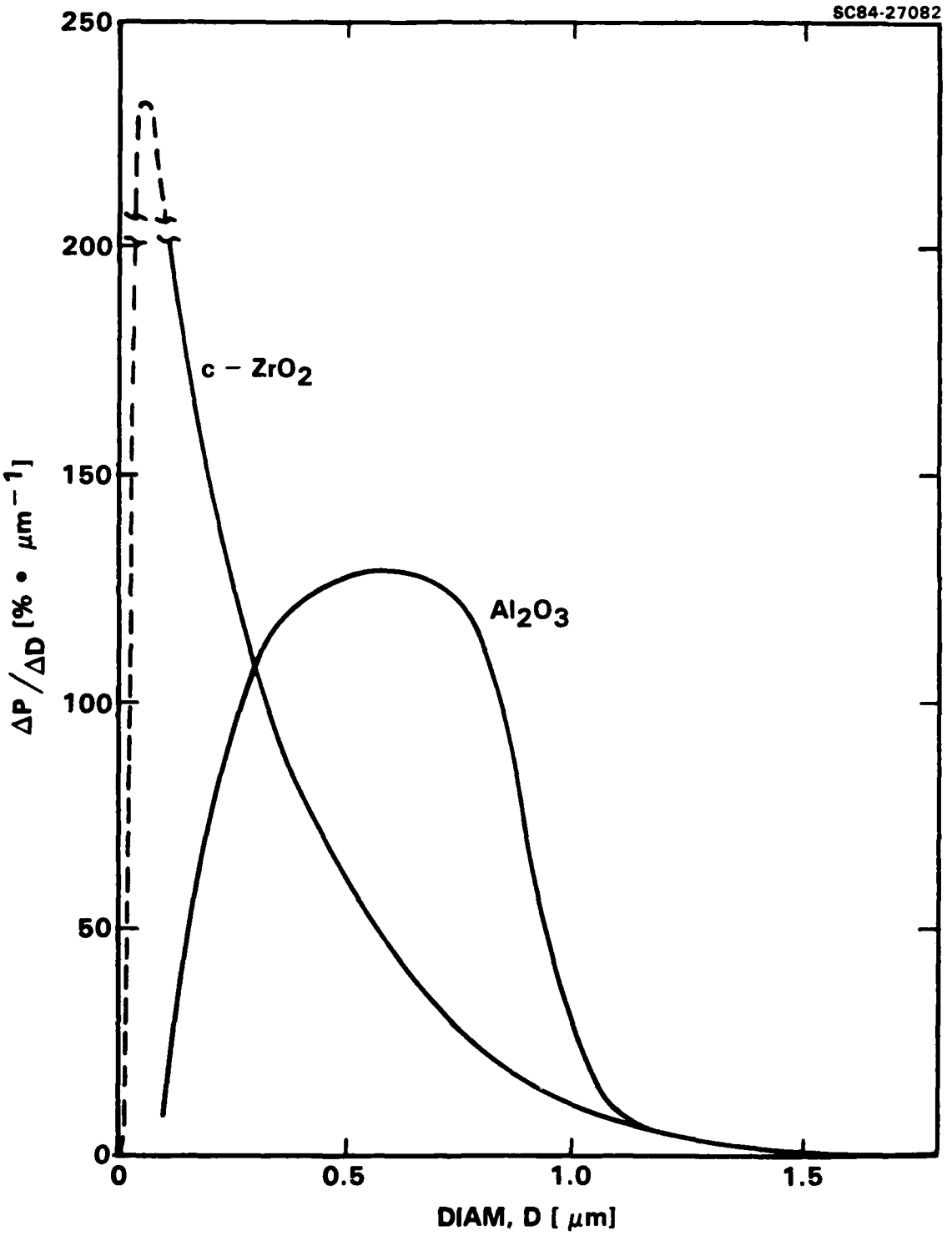

Fig. 3 Size distribution of colloidally treated Al_2O_3 and Z-ZrO_2 powders (distribution for sizes < 1 μm was not determined and is given by dashed lines).

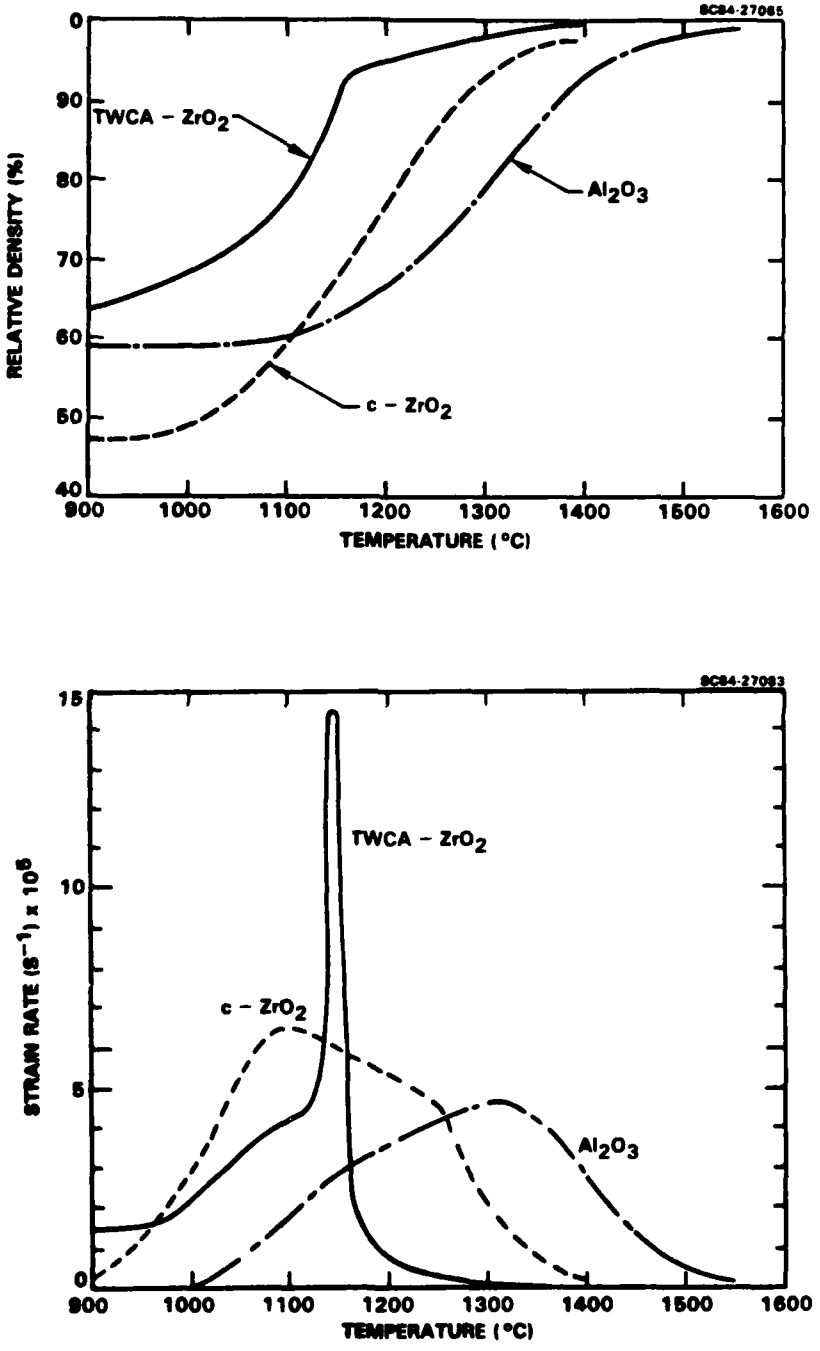

Fig. 4 Density (a) and linear strain rate (b) data vs temperature observed for the three single phase powder compacts heated at 5°C/min.

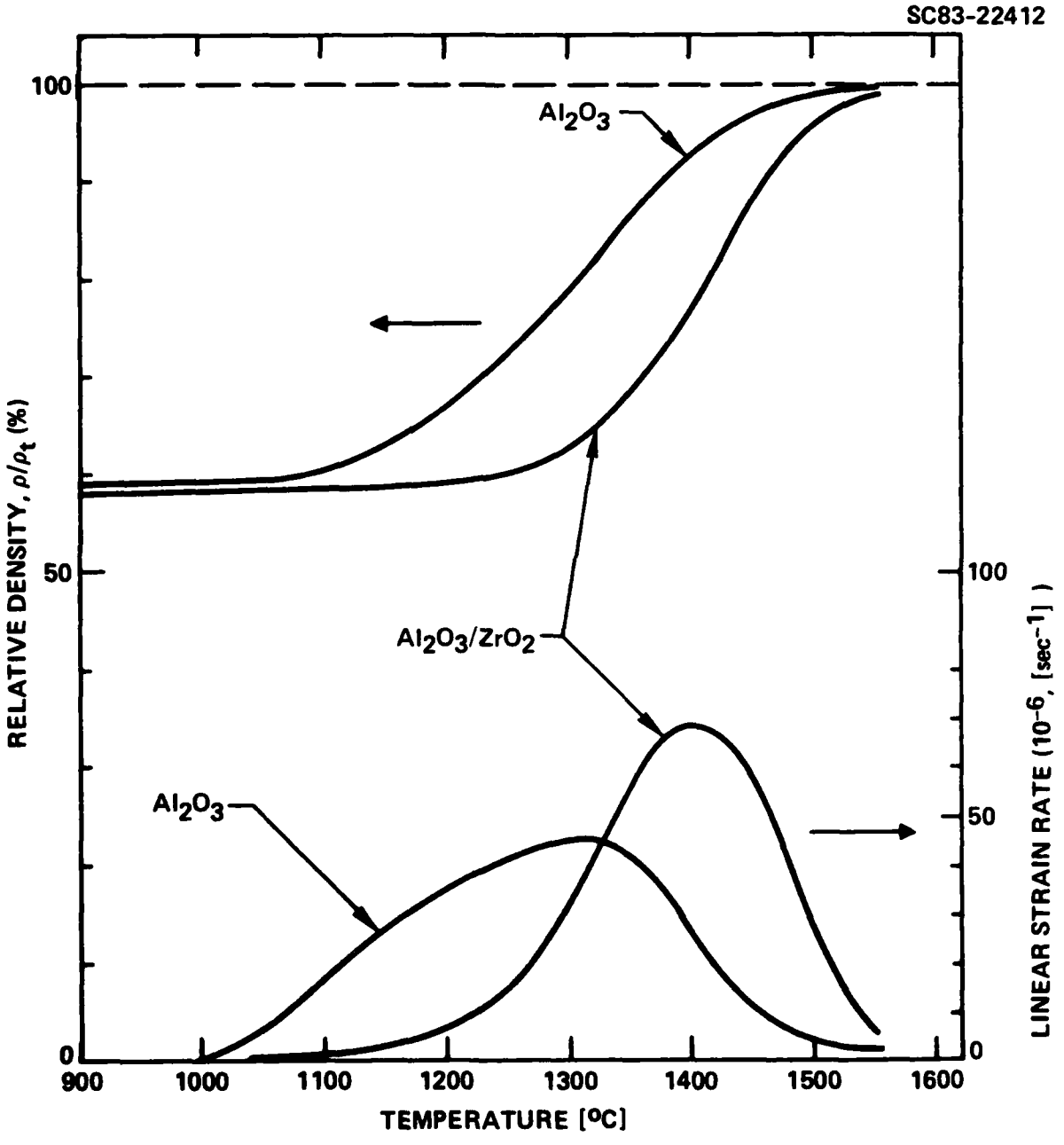

Fig. 5 Relative density and linear strain rate for the Al_2O_3 and Al_2O_3/ZrO_2 composites.

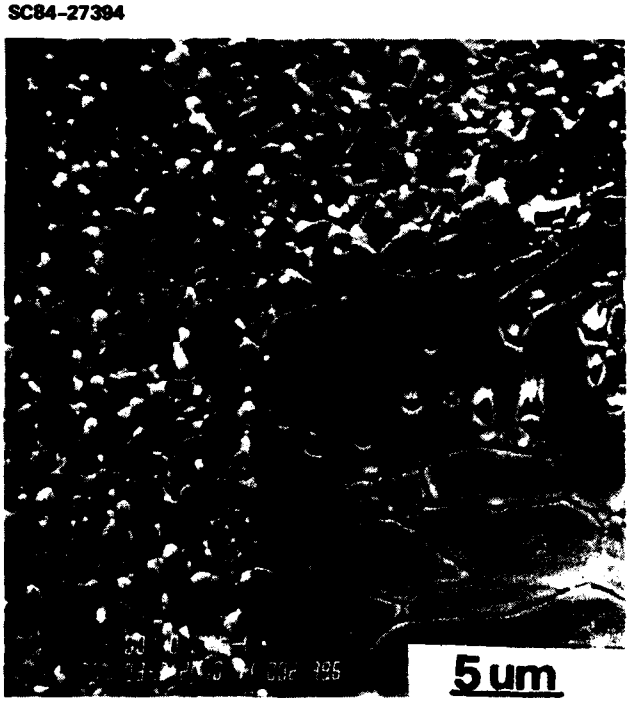

Fig. 6 Backscattered SEM micrograph of poorly mixed Al_2O_3/ZrO_2 composite sintered at 1550°C/3 hrs showing the effect of ZrO_2 (white phase/in inhibiting grain growth of Al_2O_3).

Rockwell International
Science Center

SC5368.2FR

TECHNICAL REPORT NO. 4

RELATIONS BETWEEN SHRINKAGE STRAIN, STRAIN RATE AND REARRANGEMENT DURING SINTERING: EXPERIMENTAL OBSERVATIONS WITH Al_2O_3, ZrO_2 AND Al_2O_3/ZrO_2 POWDER COMPACTS

F. F. Lange and B. I. Davis
Rockwell International Science Center
Structural Ceramics Group
Thousand Oaks, California 91360

ABSTRACT

Shrinkage strain and strain rate data were obtained at a constant heating rate for three different ZrO_2 powders, an Al_2O_3 powder and a composite Al_2O_3/ZrO_2 powder containing 2 v/o ZrO_2. All powders were colloidally treated to separate large, soft agglomerates and to remove hard agglomerates $\gtrsim$ 1 μm and then consolidated by flocced/filtration. Most powder compacts were also iso-pressed to increase bulk density. Shrinkage strains and strain rates were inversely proportional to bulk density. Mercury intrusion was used to determine the equivalent capillary size distribution at different temperatures for four different powder compacts. These data showed that larger capillaries developed as smaller capillaries disappeared during heating to a temperature near that in which the compact exhibited its maximum shrinkage strain rate. These data are consistent with previous strain calculations of symmetric multiple-particle packing units. These calculations show that shrinkage strain and strain rate is proportional to the coordination number of the pore within the packing unit and that units containing more highly coordinated pores (i.e., those that shrink more and at a faster rate) are placed in tension as the compact develops a "metastable" equilibrium configuration by short range mass transport.

1.0 INTRODUCTION

Nonperiodic arrangements of both mono- and poly-dispersed powders, spherical or otherwise, can be considered as an arrangement of different multiple-particle packing units. For the case of the random packing of identical spheres, the multiparticle packing units have been described as regular and irregular polyhedron, where spheres are centered at vertices.[1,2,3] The coordination number of the pore within each polyhedron is defined by the number of vertices. As detailed elsewhere,[4] each polyhedron's shrinkage strain and strain rate during sintering depends on its pore's coordination number. Namely, shrinkage strain and strain rate increase with coordination number. Since the powder compact can be considered a collection of different polyhedra, differential strains, strain rates and therefore, stresses will develop between the shrinking polyhedra during sintering. When one models this differential shrinkage phenomena in a manner analogous to the modeling used to explain the changing thermal expansion of polycrystals that exhibit strong crystalline anisotropy, one concludes that tensile stresses must develop within polyhedra of higher coordination numbers causing them to separate during sintering.

This process, commonly known as rearrangement, enlarges some pores at the expense of shrinking others. Namely, pores with small coordination numbers shrink and pores with large coordination numbers enlarge to increase their coordination numbers. As described previously,[3] this process of pore enlargement and the corresponding increase in the volume fraction of pores with larger coordination numbers is detrimental to densification.

Pore enlargement during rearrangement has been observed by Exner (see review in Ref. 5) during the sintering of two-directional random arrangements of spheres. Mercury porosimetry data has shown that pore enlargement occurs in many (if not all) powders during the early stages of densification.[3,6]

The purpose of the present work was to characterize the rearrangement phenomenon in relation to the shrinkage strain and strain rate of a densifying

powder compact. At the same time, the model used to explain pore enlargement in terms of the differential shrinkage of multiple-particle packing units suggested that shrinkage strain and strain rate should be inversely proportional to bulk density. Thus, experiments were also designed to examine this hypothesis.

2.0 EXPERIMENTAL

2.1 Powders, Powder Processing and Consolidation

Four different powders, viz. Al_2O_3,* ZrO_2,** ZrO_2(+2.3 m/o Y_2O_3)*** and ZrO_2(+6.6 m/o Y_2O_3),*** and one composite powder, Al_2O_3 + 0.02 volume fraction ZrO_2 (+6.6 m/o Y_2O_3) were used in this study. The four, single-phase powders had the following characteristics in the as-received state.

The Al_2O_3 powder is believed to be manufactured by atomizing an alkoxide in a manner described by Visca and Motijevic.[7] The particles were roundish and had the α-Al_2O_3 structure as determined by XRD. The as-received, dry powder contained large, soft agglomerates which could be dispersed in water (pH = 2) with ultrasonic treatment. The manufacture claims a total cation impurity content < 50 ppm. This powder was prepared for consolidation, without milling, with the colloidal treatment described below.

The undoped ZrO_2 powder (TWCA-ZrO_2) was prepared by a precipitation route from $ZrOCl_2$ and was received as an aqueous colloidal dispersion (pH = 1.8) with a ZrO_2 volume fraction of 0.04. No sediment was formed within a period of > 30 days suggesting the dispersion was free of agglomerates and that all particles were < 0.1 μm in size. X-ray diffraction analyses of the dried powder only revealed an impurity phase, NH_4Cl. This powder was simply washed to remove the excess salt as discussed below.

* Sumotomo Chemical Co. Japan (AKP-30, α-Al_2O_3).
** Teledyn-Wah Change Albany, Oregon 97321.
*** Zircar, Florida, N.Y.

The two other ZrO_2 powders, viz. ZrO_2 (+2.3 m/o Y_2O_3) (t-ZrO_2) and ZrO_2 (+6.6 m/o Y_2O_3) (c-ZrO_2) are believed to be prepared by heating cellulose, soaked with $ZrOCl_2$ and a soluble yttrium salt in air to produce the appropriate $Zr_{(1-x)}Y_xO_2 - \frac{x}{2}$ solid solution. The hard, partially sintered ZrO_2 agglomerates (see Ref. 8) produced by this heat treatment are partially milled by the manufacturer and washed to remove excess chlorine. The t-ZrO_2 powder (a mixture of monoclinic and tetragonal phases) was obtained as a centrifuged, wet cake and prepared for consolidation without milling, with the colloidal treatment described below. The c-ZrO_2 (cubic ZrO_2) was obtained as a dry powder and was prepared by dispersing in deionized water (pH = 2) and ball milling with a high purity Al_2O_3 milling media and jar.* The large (5 to 25 μm) Al_2O_3 particles introduced during milling were removed in the sedimentation step of the collidal treatment described below.

The colloidal treatment, designed to separate soft agglomerates and remove large, hard agglomerates is schematically outlined in Fig. 1. The treatment consisted of dispersing the powder in water at a volume fraction < 0.04, with sufficient HCl to maintain a pH of 2, sedimenting to remove hard agglomerates (assumed to be dense spherical particles) > 1 μm and floccing the retained dispersion with NH_4OH to increase the pH to ~ 8. Floccing increased the volume fraction of solid and prevented mass segregation during storage. The flocced slurry was washed three times to remove excess salts by removing the clear supernate, adding deionized water, and refloccing without acid or base additions.

With the exception of the TWCA-ZrO_2 powder, the particle size distribution was determined** after redispersing the single-phase flocced slurries.

The Al_2O_3/ZrO_2 composite containing 2 v/o c-ZrO_2 was prepared by first redispersing the flocced single-phase slurries (decreasing pH to 2),

* Coores Porcelain Co.
** Micromeritics Sedigraph 5000D

measuring their densities to determine their solid contents, and then mixing the appropriate weight fractions with the aid of an ultrasonic horn. Once mixed, the two-phase dispersion was immediately flocced to preserve the uniform phase distribution of the dispersed state.

All flocced slurries were consolidated by filtering (slip casting) in cylindrical teflon molds on casting plaster. After drying, some specimens were iso-pressed at 350 MPa to increase the initial bulk density.

Sintering experiments were carried out at a constant heating rate of 5°C/min at a temperature up to 1400°C for the ZrO_2 powder compacts and 1550°C for the Al_2O_3 and Al_2O_3/ZrO_2 powder compacts. A high temperature extensometer, described elsewhere,[9] was used to measure linear shrinkage during heating. Shrinkage was continuously recorded as a function of time. The final density, determined by the Archimedes method, and the initial bulk density were compared with the total recorded shrinkage to insure the accuracy of the linear shrinkage measurements. Density was calculated as a function of temperature (ρ_T) using the relation $\rho_T = \rho_o\ (1-\varepsilon)^{-3}$, where ρ_o = the initial bulk density and ε = the linear shrinkage strain at the desired temperature. Linear shrinkage strain rates were determined as a function of temperature using a programmer .....

An automated, mercury porosimeter,* was used to determine the equivalent capillary size distribution of the connected porosity as a function of sintering temperature. Data were obtained at different intrusion pressures after a 30 s equilibration at each incremental pressure increases. The surface energy/unit area of the mercury and its contact angle with each solid were assumed to be 484 dyne/cm^2 and 130°, respectively. Specimens used for these experiments were cast at the same time as those used for the densification study, but were separately heated to the desired temperature. The mercury porosimeter was also used to determine the initial bulk density of each powder compact.

* Micrometrics Auto-Pore 9200.

3.0 RESULTS

3.1 Size Distributions

Figure 2 illustrates the size distribution of the three single-phase powders which could be measured (a distribution for the TWCA-ZrO_2 could not be obtained with the instrument since all particles and/or agglomerates were < 0.1 μm). The dashed lines in Fig. 2 indicate the expected distribution for sizes <0.1 μm. The two peaks for the t-ZrO_2 distribution suggests two separate distributions, viz., the peak at ~ 0.7 μm suggests a distribution due to hard agglomerates and the peak at < 0.1 μm suggests a distribution due to single particles. The distribution for the c-ZrO_2, manufactured by the same method as the t-ZrO_2, but milled prior to sedimentation, indicates that milling broke down many of the hard agglomerates.

3.2 Densification Data

The relative density and shrinkage strain rate data for the four single phase powder compacts, each with two initial bulk densities are illustrated in Figs. 3 through 5. For all powders examined, the shrinkage strain (illustrated in the figures as relative density) and strain rate was greater for compacts with a lower initial bulk density. Figure 5 also contains the densification data for the iso-pressed, Al_2O_3/ZrO_2 composite compact. The strain rate data for both the c-ZrO_2 (Fig. 3) and t-ZrO_2 (Fig. 4) compacts indicate two maximum, suggesting the shrinkage of two types of multiple-particle packing units, e.g., lower density units formed by single particles and higher density, hard agglomerates.* This reasoning is consistent with the observations of Rossen and Hausner,[10] who have shown that agglomerates can produce a separate strain rate maximum relative to their surrounding matrix. For the more agglomerated t-ZrO_2 powder, the low temperature maximum signifi-

* The initial relative bulk density of the ZrO_2 hard agglomerates has been estimated to be ~ 0.40.[8]

cantly diminishes with increased initial bulk density, suggesting that the higher temperature maximum in both the c- and t-ZrO_2 compacts is produced by the higher density, hard agglomerates.

Bulk densification initiated at 300°C for the amorphous, TWCA-ZrO_2 powder compacts (not shown in Fig. 5). Some of this low temperature densification may be a result of crystallization. These powder compacts had the most pronounced strain rate maximum relative to the other powder compacts.

The addition of 2 v/o ZrO_2 to Al_2O_3 delayed bulk densification of the Al_2O_3 by ~ 100°C. As detailed elsewhere,[11] addition of 10 v/o ZrO_2 produce nearly identical results. The effect of ZrO_2 in inhibiting the sinterability of Al_2O_3 has been attributed to the fact that ZrO_2 also inhibits the grain growth of Al_2O_3.

3.3 Equivalent Capillary Distributions

Mercury intrusion data were obtained at different temperatures for the flocced/filtered and flocced/filtered/iso-pressed c-ZrO_2 (Fig. 7 and 8) compacts and the flocced/filtered/iso-pressed Al_2O_3 (Fig. 9) and Al_2O_3/ZrO_2 (Fig. 10) compacts. These data, represented by Figs. 7 through 10 as bar graphs, which reflect the incremental pressure steps, show the disappearance of the smallest equivalent capillaries and the development of larger equivalent capillaries during the initial stage of heating. When the data are correlated to the densification data (Figs. 3 and 6), it can be seen that the redistribution of void space to produce large equivalent capillaries occurs prior to and during initial bulk shrinkage and stops near the temperature which the densifying compact exhibits its maximum shrinkage strain rate. At temperatures exceeding the maximum shrinkage strain rate, the larger equivalent capillaries produced at lower temperatures disappear to form smaller capillaries.

Figures 7 and 8 also show that iso-pressing eliminates a portion of the void space associated with the larger capillaries to increase bulk density (viz. 0.32 to 0.49% relative density) and redistributes the rest to produce a larger fraction of smaller capillaries.

4.0 DISCUSSION

The major observations of this work are that the shrinkage strain and strain rate of a powder compact are inversely proportional to the initial bulk density and that the rearrangement of void space (disappearance of smaller voids and the formation of larger voids) takes place prior to the maximum shrinkage strain rate. As discussed below, both of these observations are consistent with the model proposed to relate the sintering behavior of multiple-particle packing units to the densification behavior of a compact formed of different multiple-particle packing units.

As detailed elsewhere,[4] the shrinkage strain of a symmetric multiple particle packing unit (e.g., a two-dimensional ring of spheres or a three-dimensional polyhedral packing of spheres) each containing a single 'pore' formed with identical spheres depends on both the dihedral angle (i.e., ratio of surface and grain boundary energies) and the number of spheres within the packing unit. Attainment of metastable configuration of such units (i.e., no grain growth) only requires short-range, inter-particle diffusion. During mass transport, the pore within the unit shrinks but only disappears when the sums of the diehedral angle and the angle subtended by the particle is $> \Pi$. Grain growth induced by either different sphere sizes and/or an asymmetry in the packing arrangement can produce pore closure, but requires longer range, intra-particle diffusion.

The analysis of the symmetric packing unit shows that the greater the number of spheres that form the unit (i.e., the greater the pore's coordination number), the greater the shrinkage strain (an obvious conclusion). Less obvious is the result that since shrinkage of the unit only depends on inter-particle mass transport, the time required to achieve a metastable configuration is independent of the number of spheres that form the unit. That is, the time required to achieve a metastable configuration is the same for two spheres and a packing unit of many spheres. Thus, since the shrinkage strain increases with the number of particles, the shrinkage strain rate will

increase in the same manner, viz. units with more particles (containing more highly coordinated pores) will shrink more and at a faster rate.

When one approximates a powder compact with the packing of different symmetric multiple-particle packing units one must conclude that the average shrinkage strain and strain rate will be inversely related to the initial bulk density. Namely, lower bulk density compacts must be formed with larger average packing units (units containing a pore with more coordinating particles) which will exhibit a greater shrinkage strain and strain rate. In addition, since the shrinkage of an individual packing unit must be constrained by the mean shrinkage (i.e., the shrinkage of the powder compact), differential strains, strain rates and therefore stresses must arise between the different units. Larger units will be placed in tension and smaller units in compression. This reasoning suggests that the units containing a higher coordinated pore will separate during the rearrangement stage of sintering and that this rearrangement process will take place during the early stages of sintering when the multiple particle packing attempt to reach a metastable equilibrium configuration by a short-range diffusional process.

Using this conceptual model of a powder compact one might explain the major experimental observation of this work. First, the lower bulk density flocced/filtered compacts must contain, on the average, larger multiple packing units, viz., units with more highly coordinated pores. As observed by the capillary size distribution data, iso-pressing decreases the average packing unit size (units containing a pore with few coordinating particles). Thus, the iso-pressed compacts will exhibit less shrinkage and a smaller shrinkage strain rate.

Second, one might interpret the temperature of maximum strain rate as the temperature where most multiple-particle packing units have acquired a "metastable" configuration by short range diffusion. Prior to reaching this temperature, differential shrinkage strains and strain rates cause larger packing units to separate as the smaller units densify thus redistributing void space to produce larger and lower coordinated pores. This process is

expected to produce a dense skeletal structure at (or near) the temperature of maximum strain rate. Further densification of this skeletal structure requires either longer range diffusion phenomena (hence smaller strain rates) or creep deformation by an applied stress (e.g., hot-pressing).

5.0 REFERENCES

1. J.D. Bernal, "The Bakerian Lectures, 1962: The Structure of Liquids," Proc. R. Soc. (London, Ser. A., 280, 299 (1964).

2. H.J. Frost, "Overview 17: Cavities in Dense Random Packing," Acta Metall. 30[5] 889-904 (1982).

3. F.F. Lange, "Sinterability of Agglomerated Powders," J. Am. Ceram. Soc. 67, 83-89 (1984).

4. B. Kellett and F.F. Lange, to be published.

5. H.E. Exner, "Principles of Single Phase Sintering," Rev. Powder Metall. Phys. Ceramics 1[1-4], 1-251 (1979).

6. O.J. Whittemore, Jr. and J.J. Sipe "Pore Growth During the Initial Stages of Sintering Ceramics," Powder Technol. 9, 159 (1974).

7. M. Visca and E. Matijevic, "Preparation of Uniform Colloidal Dispersions by Chemical Reactions in Aerosols," J. Colloidal and Interface Sci. 68[2], 308-19 (1979).

8. F.F. Lange, B.I. Davis and I.A. Aksay, "Processing-Related Fracture Origins: Part III," J. Am. Ceram. Soc. 66[6], 407-8 (1983).

9. F.F. Lange, B.I. Davis and D.R. Clarke "Compressive Creep of Si_3N_4/MgO Alloys: Part I," J. Mat. Sci. 15, 600-610 (1980).

10. A. Rossen and H. Hausner, "Sintering Kinetics of ZrO_2 Powders," Ceramic Advances.

11. F.F. Lange, T. Yamaguchi, B.I. Davis and P.E.D. Morgan, "Effect of ZrO_2 Inclusions on the Sinterability of Al_2O_3," to be published.

ACKNOWLEDGEMENTS

This work was supported by the Office of Naval Research under Contract No. N00014-83-C-0469.

TWO-PHASE MIXTURES

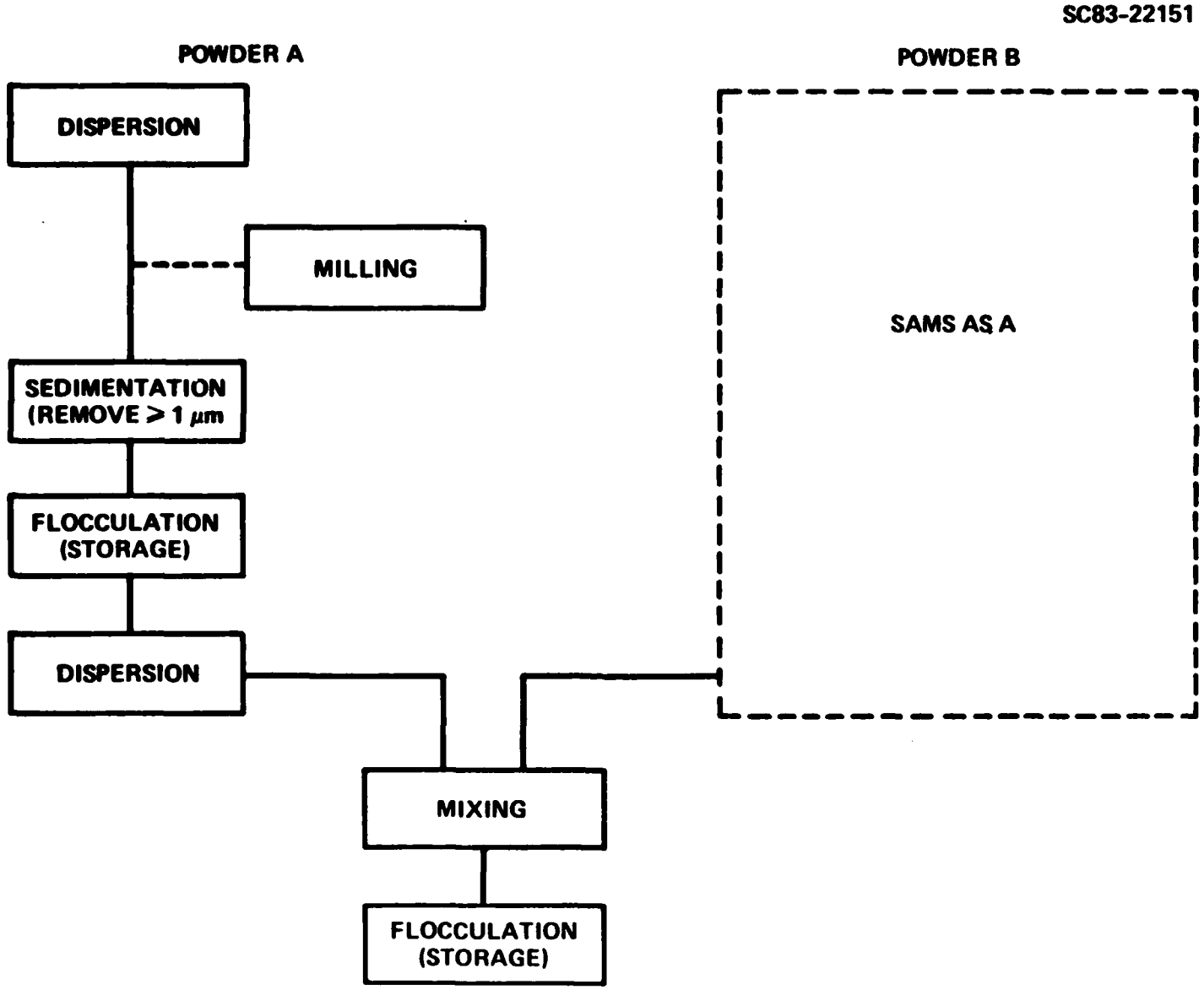

Fig. 1 Schematic for colloidal preparation of single-phase and multiphase powders to minimize soft and hard agglomerate size.

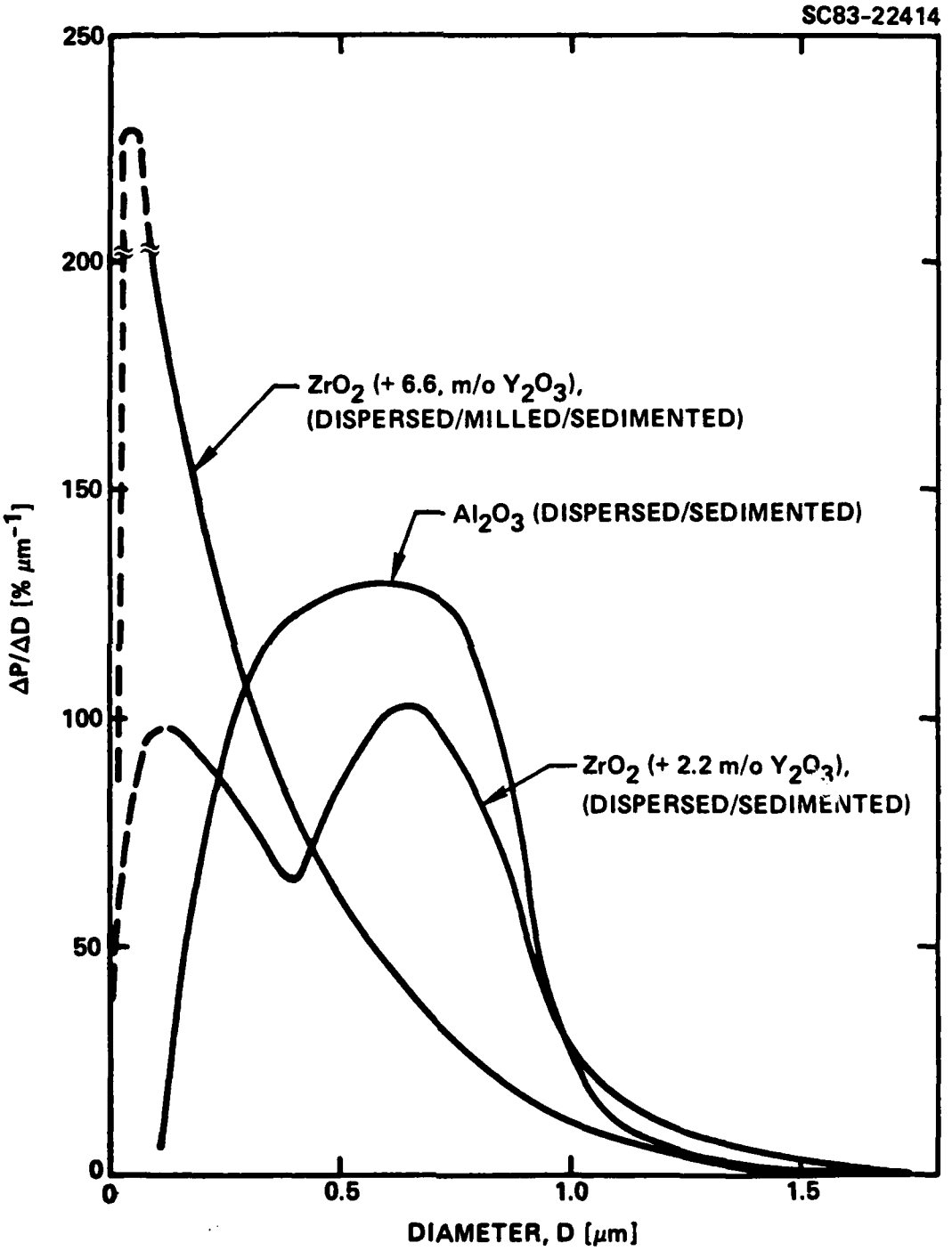

Fig. 2 Size distribution of the colloidally treated single-phase powders used for this study (excluding the precipitated TWCA-ZrO_2 powder).

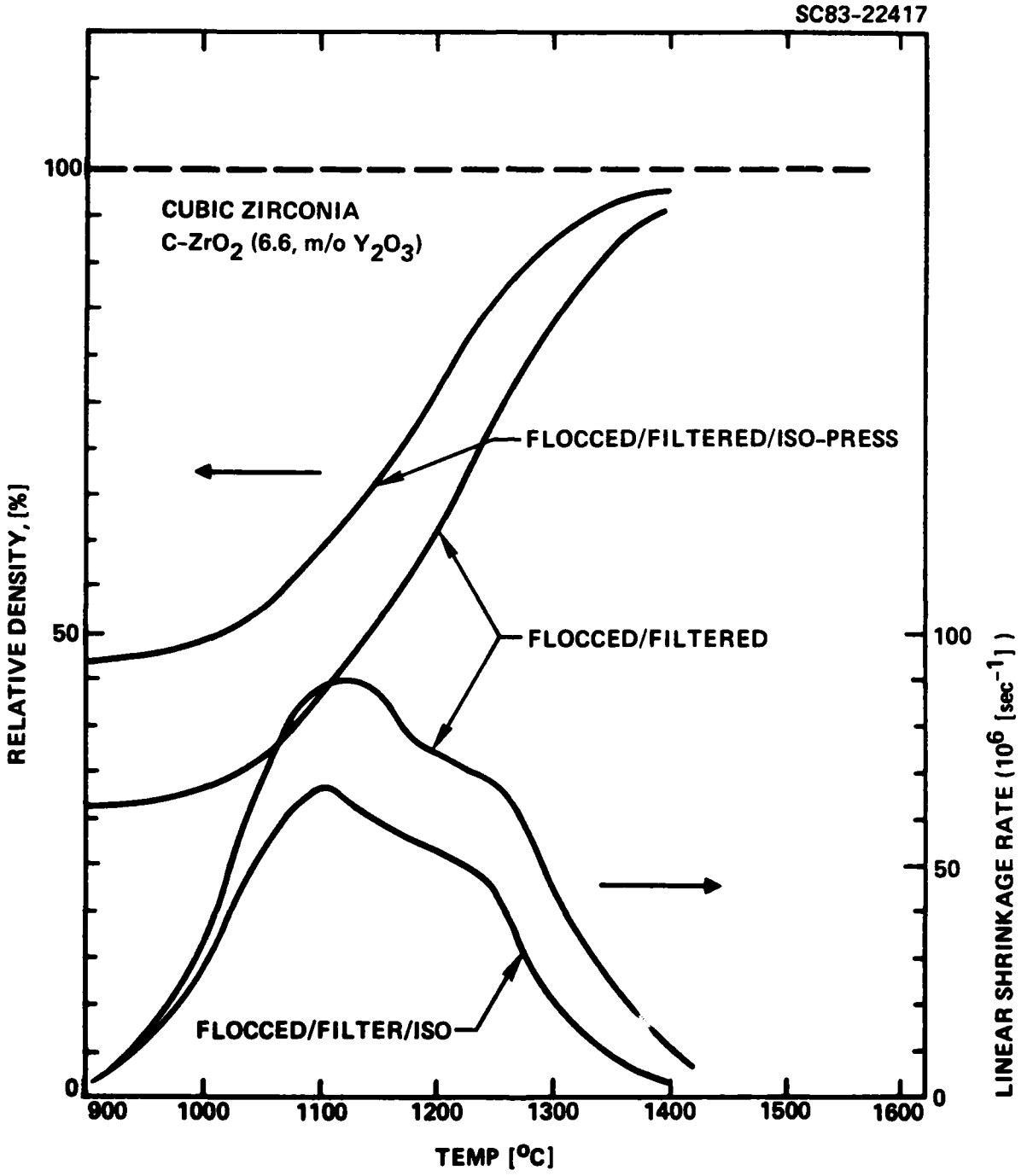

Fig. 3 Relative density and shrinkage strain rate vs temperature (heating rate = 5°C/min) for the c-ZrO_2 powder compacts.

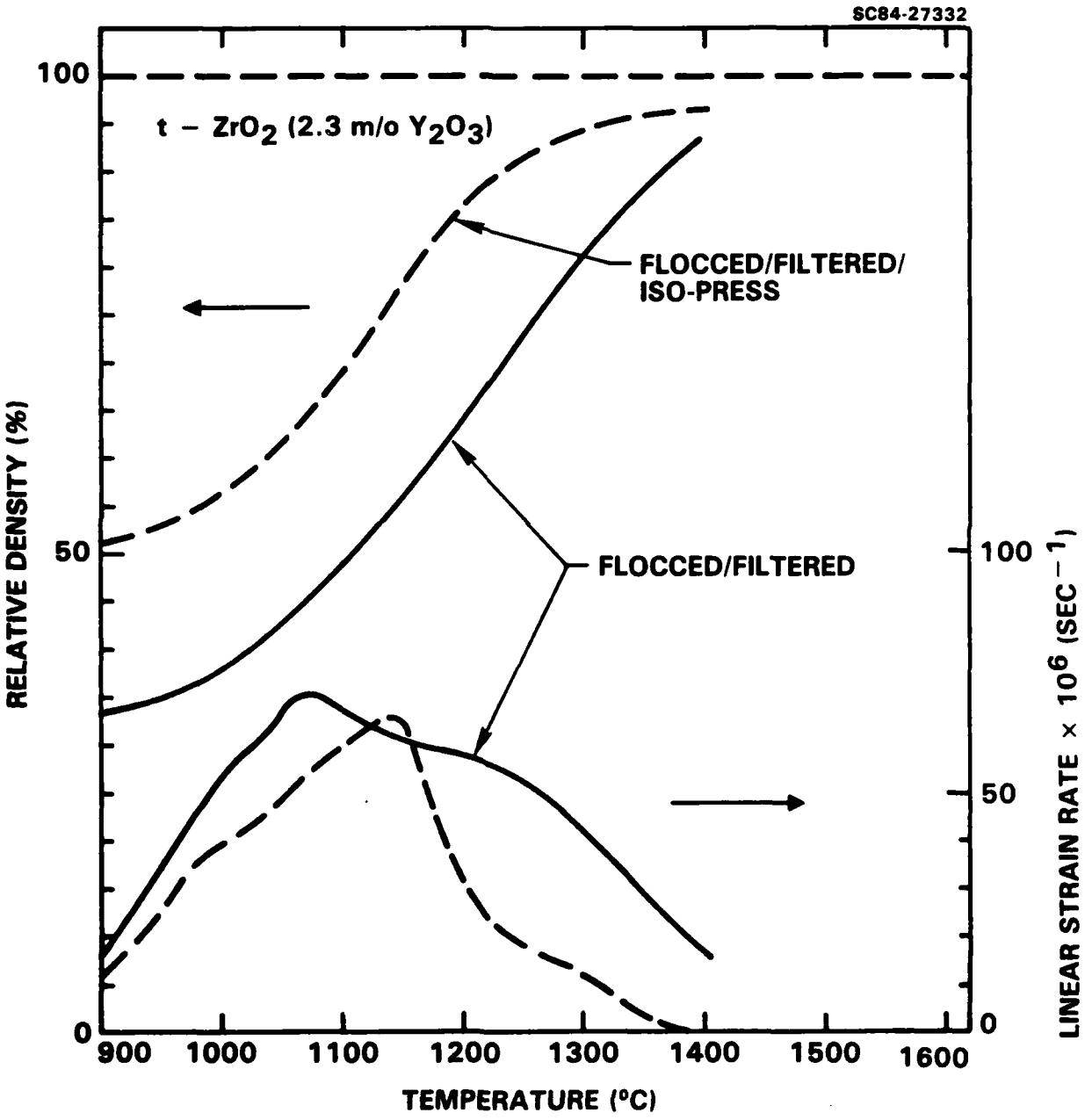

Fig. 4 Relative density and shrinkage strain rate vs temperature (heating rate = 5°C/min) for the t-ZrO_2 powder compacts.

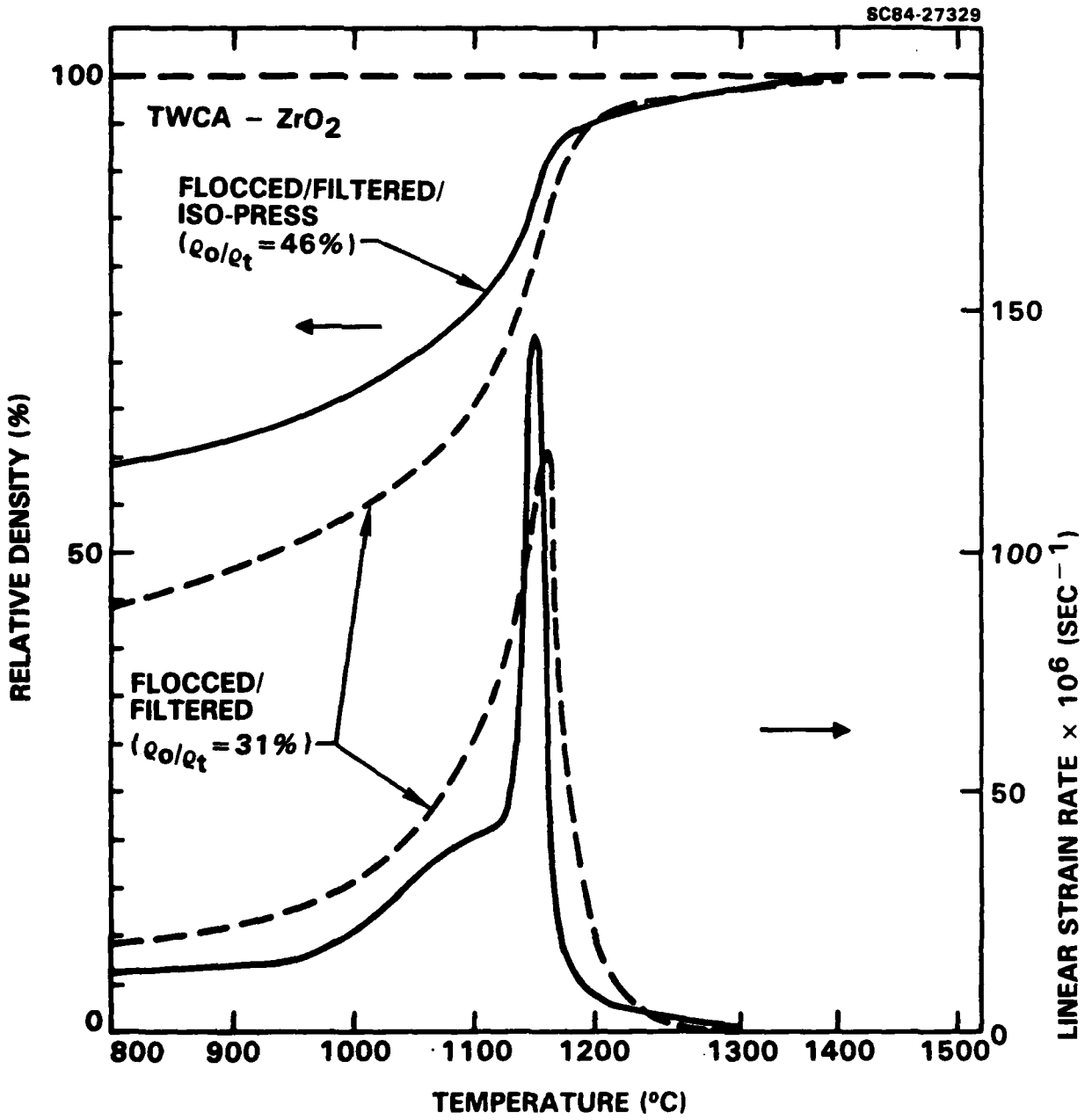

Fig. 5 Relative density and shrinkage strain rate vs temperature (heating rate = 5°C/min) for the TWCA-ZrO_2 powder compacts.

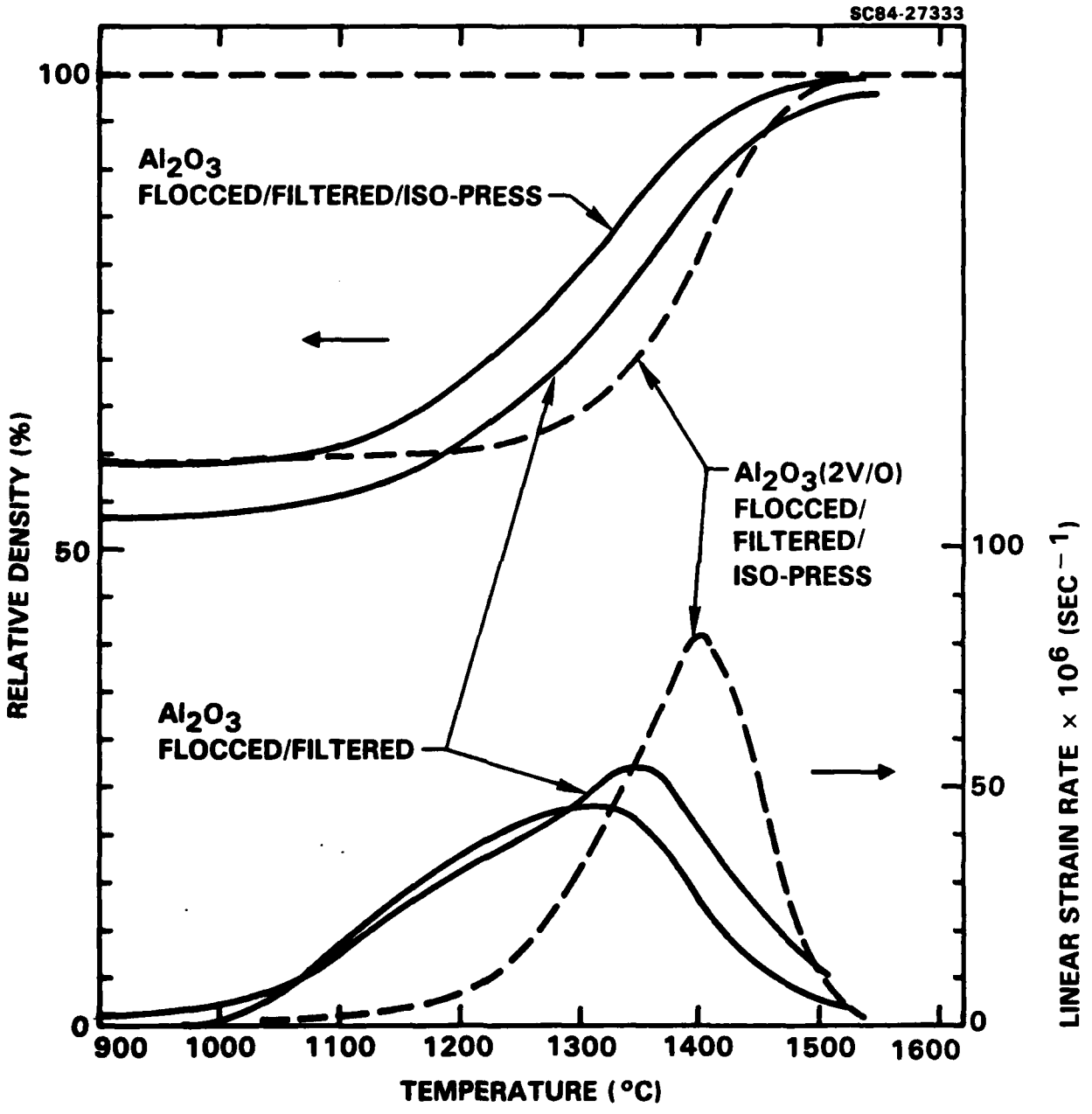

Fig. 6 Relative density and shrinkage strain rate vs temperature (heating rate = 5°C/min) for the Al_2O_3 and Al_2O_3/ZrO_2 (2 v/o) powder compacts.

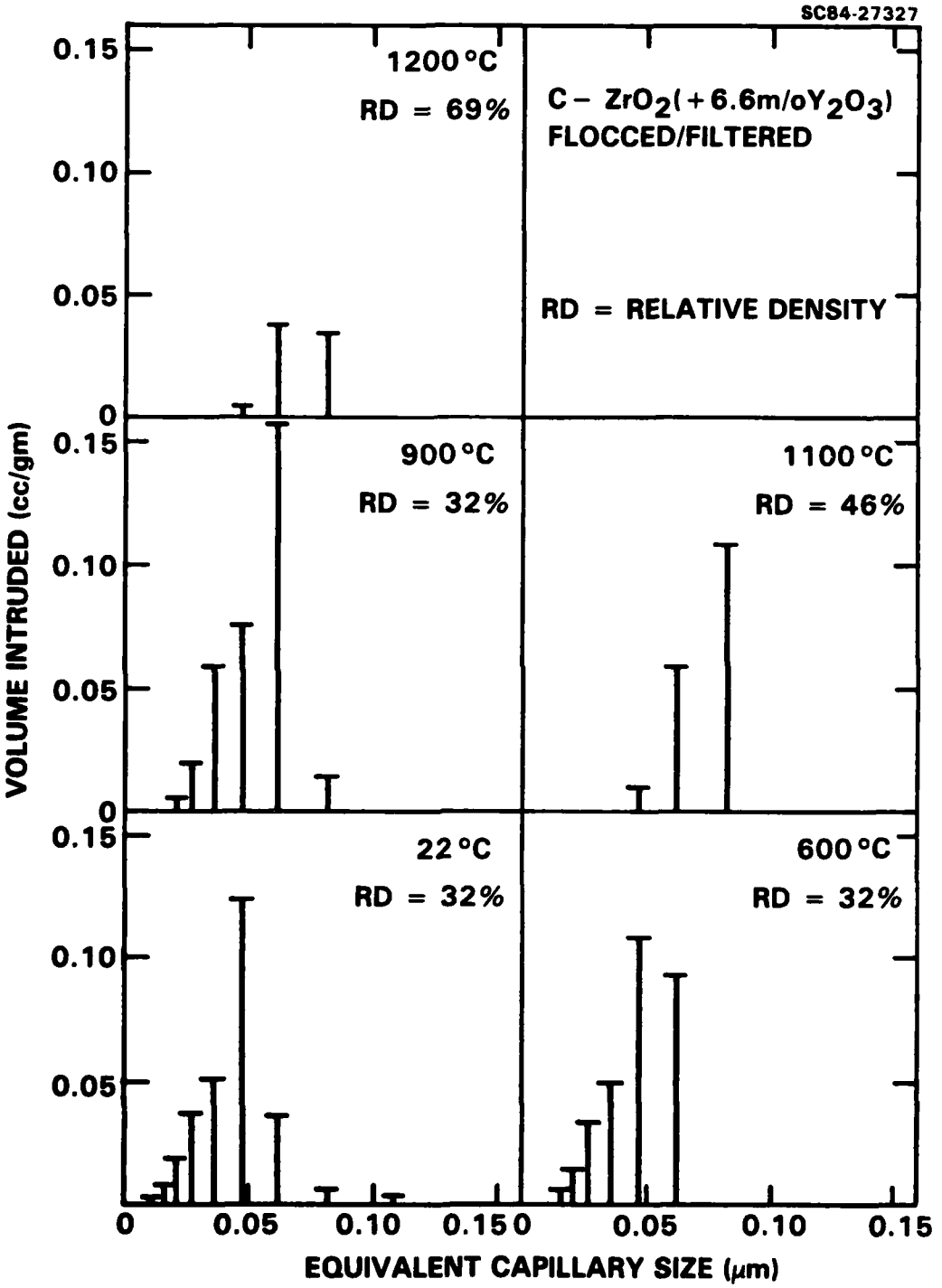

Fig. 7 Equivalent capillary size distributions determined by incremental mercury intrusion for the flocced/filtered c-ZrO_2 compacts.

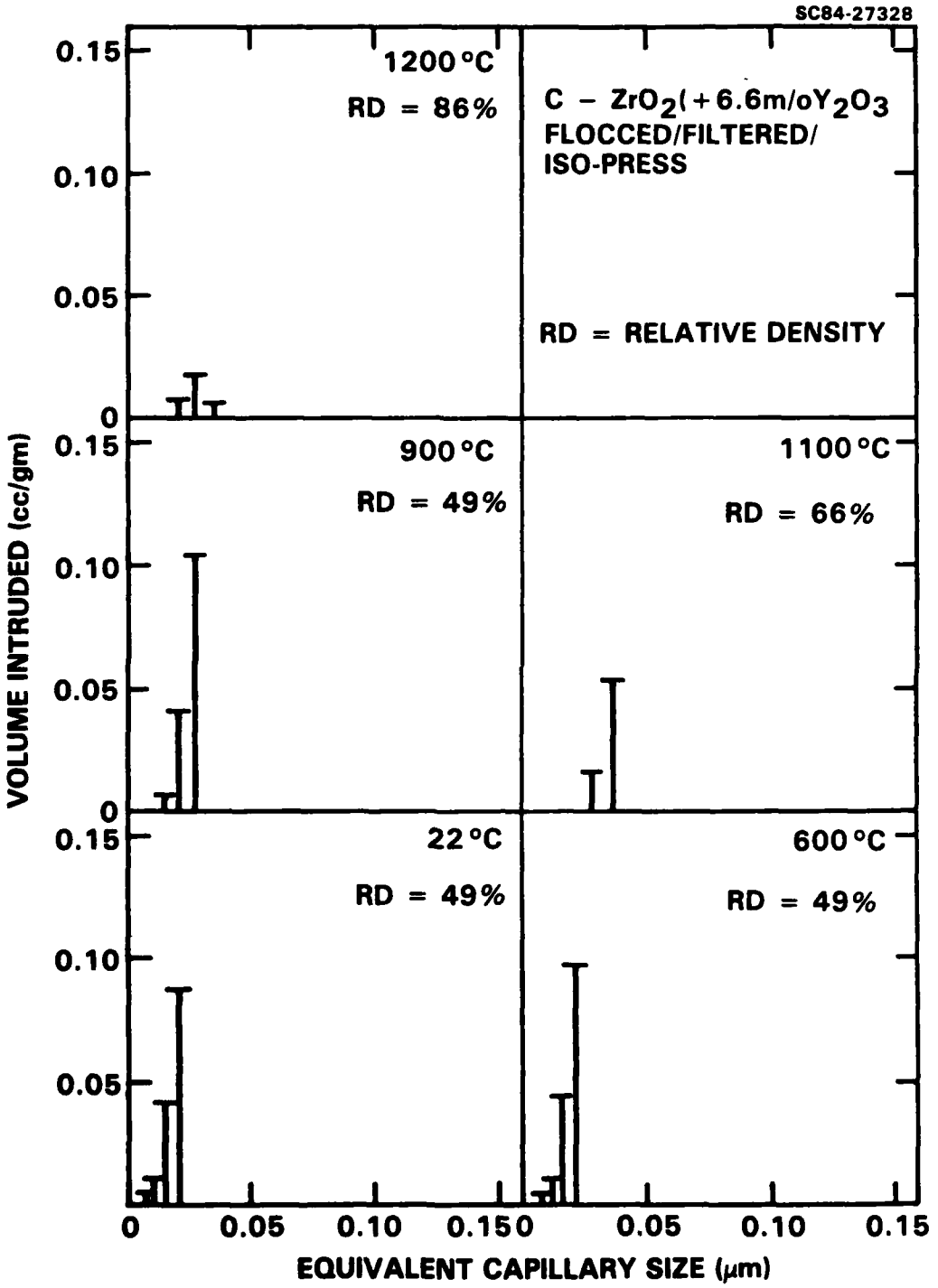

Fig. 8 Equivalent capillary size distributions determined by incremental mercury intrusion for the flocced/filtered/iso-pressed c-ZrO_2 compacts.

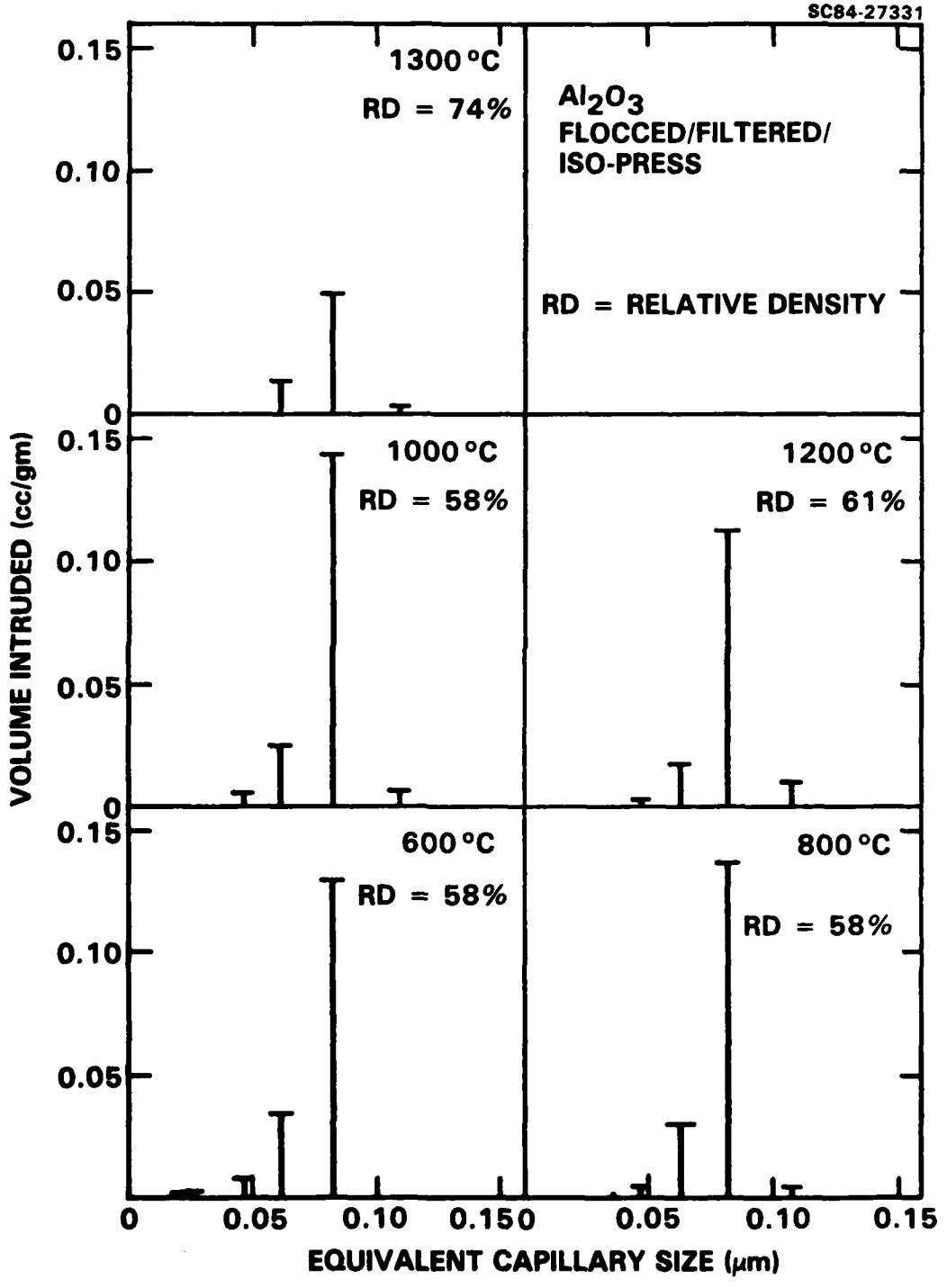

Fig. 9 Equivalent capillary size distributions determined by incremental mercury intrusion for the flocced/filtered iso-pressed Al_2O_3 compacts.

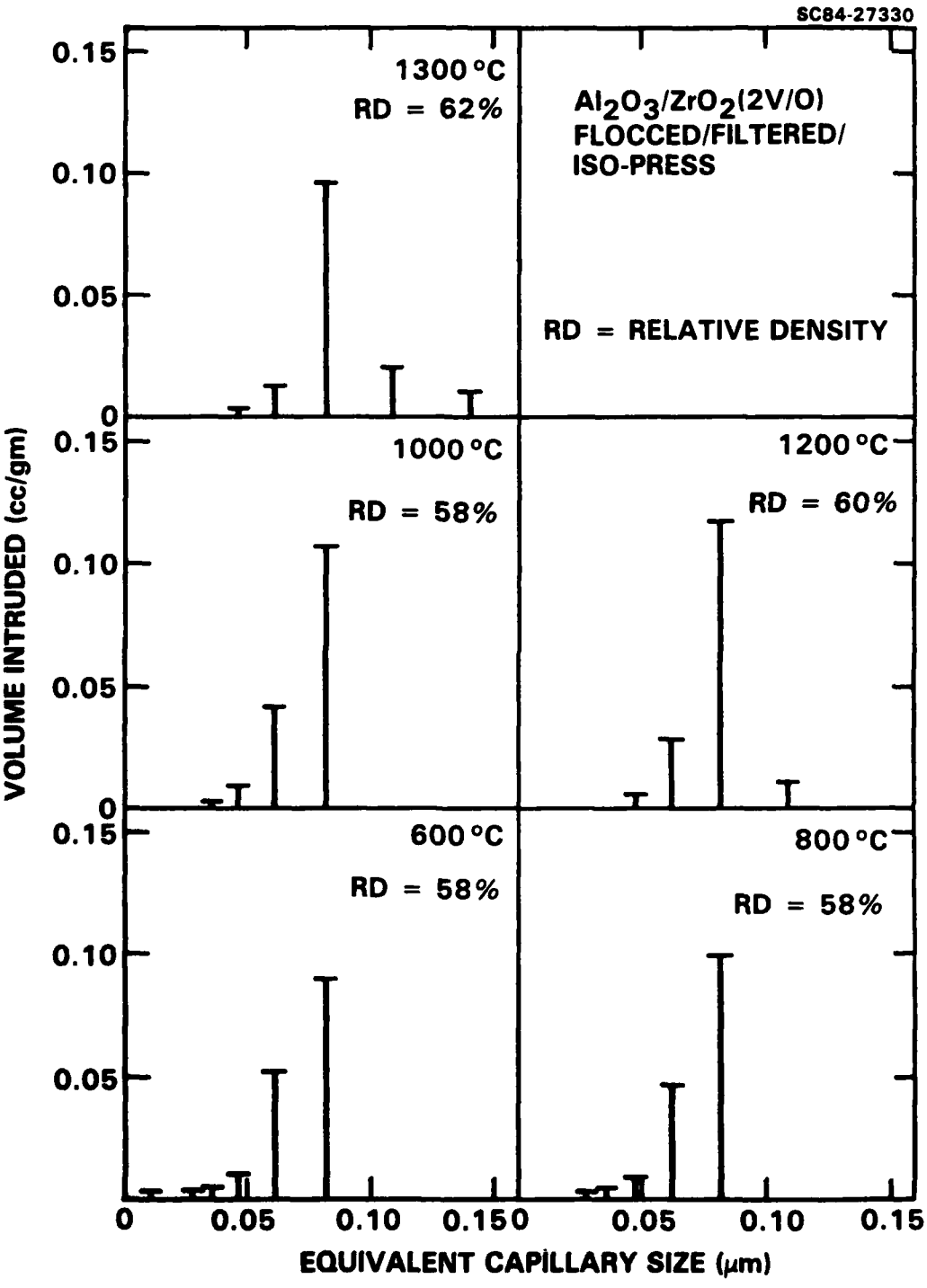

Fig. 10 Equivalent capillary size distributions determined by incremental mercury intrusion for the flocced/filtered/iso-pressed Al_2O_3/ZrO_2 (2 v/o) compacts